MOLECULAR AND CELLULAR BIOLOGY, Dec. 1995, p. 6670–6685 Vol. 15, No. 12
0270-7306/95/$04.00+0


# Initiation Binding Receptor, a Factor That Binds to the Transcription Initiation Site of the Histone *h5* Gene, Is a Glycosylated Member of a Family of Cell Growth Regulators

ALICIA GÓMEZ-CUADRADO, MERCÈ MARTÍN, MICHELINE NOËL, AND ADOLF RUIZ-CARRILLO*

*Cancer Research Center and Department of Biochemistry, Medical School of Laval University, L'Hôtel-Dieu de Québec, Québec, Québec G1R 2J6, Canada*

Received 2 June 1995/Returned for modification 1 August 1995/Accepted 28 August 1995

**Initiation binding receptor (IBR) is a chicken erythrocyte factor (apparent molecular mass, 70 to 73 kDa) that binds to the sequences spanning the transcription initiation site of the histone *h5* gene, repressing its transcription. A variety of other cells, including transformed erythroid precursors, do not have IBR but a factor referred to as IBF (68 to 70 kDa) that recognizes the same IBR sites. We have cloned the IBR cDNA and studied the relationship of IBR and IBF. IBR is a 503-amino-acid-long acidic protein which is 99.0% identical to the recently reported human NRF-1/α-Pal factor and highly related to the invertebrate transcription factors P3A2 and erected wing gene product (EWG). We present evidence that IBR and IBF are most likely identical proteins, differing in their degree of glycosylation. We have analyzed several molecular aspects of IBR/F and shown that the factor associates as stable homodimers and that the dimer is the relevant DNA-binding species. The evolutionarily conserved N-terminal half of IBR/F harbors the DNA-binding/dimerization domain (outer limits, 127 to 283), one or several casein kinase II sites (37 to 67), and a bipartite nuclear localization signal (89 to 106) which appears to be necessary for nuclear targeting. Binding site selection revealed that the alternating RCGCRYGCGY consensus constitutes high-affinity IBR/F binding sites and that the direct-repeat palindrome TGCGCATGCGCA is the optimal site. A survey of genes potentially regulated by this family of factors primarily revealed genes involved in growth-related metabolism.**

Histone H5 is a specific linker histone of the erythroid lineage which is expressed during the maturation of embryonic and adult avian erythrocytes (reference 2 and references therein). The chromatin levels of H5 increase progressively following activation of the *h5* gene, so that at the end of the maturation process, the stoichiometry of linker histones (H5 plus H1) per core histone octamer is more than 1 (5). The effects of ectopic expression of H5 in nonerythroid cells, to levels comparable to those found in erythrocytes, argues for a direct role of H5 in the condensation and inactivity of the erythrocyte nucleus (81, 82).

Although the *h5* gene is already set in an active chromatin conformation in early erythroid precursors (69), its transcription is not activated until the preerythroblast-to-erythroblast transition (2, 72), coincident with the decline in the proliferation potential of the cells. The mechanisms that bring about transcriptional activation of the *h5* gene are not fully elucidated but appear to reflect alterations in the balance between positive and negative effectors. Transcription of the *h5* gene is regulated by a complex assortment of ubiquitous and blood cell-specific factors acting at the promoter and three differentiation-specific enhancers located upstream and downstream of the gene (72, 73). Although the majority of these factors contribute to transcriptional activity, one of them, IBR, was found to repress *h5* transcription in vitro (25). IBR from immature and mature adult erythrocyte nuclei is a protein with an apparent molecular mass of 70 to 73 kDa that specifically binds to the GC-rich sequences spanning the transcription initiation site of the *h5* gene. IBR repression of *h5* transcription appears to occur by interference with the assembly of the transcription initiation complex (25).

IBR was not found in HD3 cells (avian erythroblastosis virus [AEV]-transformed erythroid precursors), which instead contain a protein of 68 to 70 kDa that recognized the IBR sites of the *h5* gene with a similar degree of specificity (25). Our previous work did not distinguish whether IBR was a maturation-specific form of IBF or a different protein expressed in maturing erythrocytes. We report here the cloning of IBR cDNA and present evidence indicating that IBR and IBF are differentially glycosylated products of the same gene. IBR/F is a member of a family of evolutionarily related transcription factors that includes sea urchin P3A2 (11), the *Drosophila* erect wing gene product (EWG) (17), and the recently reported human NRF-1/α-Pal factor (18, 88). The invertebrate members of this family have been implicated in the regulation of genes involved in the development of muscle and the central nervous system. In vertebrates, they have been shown to activate transcription of genes involved in mitochondrial energy transduction (88) and protein synthesis (18). We argue that these factors play a role in the regulation of growth-related metabolism.

We also present a structural analysis of IBR/F and show that it associates as stable homodimers and that the dimer is the relevant DNA-binding species. Our results also show that the N-terminal half of the protein, harboring the DNA-binding/dimerization domain, the necessary nuclear localization signal (NLS), and several potential casein kinase II (CK-II) sites, has been conserved during evolution, whereas the C-terminal half has diverged considerably. A detailed study of the transcriptional effect of IBR and IBF on the *h5* gene will be presented in a separate communication (24a).

## MATERIALS AND METHODS

**Nuclear extracts and factor purification.** Nuclear extracts and IBR from $5 \times 10^{11}$ mature hen erythrocytes were prepared as described before (25). IBF was obtained from $1.5 \times 10^{11}$ HD3 cells essentially as described before (25) with the

* Corresponding author. Phone: (418) 691-5550. Fax: (418) 691-5439. Electronic mail address: Adolf.Ruiz-Carrillo@bcx.ulaval.ca.

following modifications. The nuclear extract in buffer A (25 mM HEPES [*N*-2-hydroxyethylpiperazine-*N*′-2-ethanesulfonic acid, pH 7.9], 20% glycerol, 3 mM $MgCl_2$, 10 μM $ZnCl_2$, 0.2 mM EGTA [ethylene glycol tetraacetic acid], 6 mM 2-mercaptoethanol, 5 mM β-glycerophosphate, 0.5 mM phenylmethylsulfonyl fluoride [PMSF], 1 μM leupeptin, 1 μM pepstatin) containing 0.3 M KCl was chromatographed through a 35-ml heparin-agarose column (Pharmacia) with a 0.3 to 0.6 M KCl gradient in buffer A. The 0.4 to 0.5 M KCl fractions were pooled, dialyzed against 0.2 M KCl in buffer A, and loaded in a 5-ml wheat germ agglutinin (WGA)-Sepharose 4B column. The flowthrough was loaded in a 10-ml double-stranded DNA-cellulose column (Sigma) and eluted with a 0.2 to 0.6 M KCl gradient in buffer A. The 0.5 M KCl fraction containing IBF was further purified by two rounds of affinity chromatography with oligomerized cognate oligonucleotides bound to Sepharose. For columns containing the histone *h5* sequence, the sample was loaded in 0.2 M KCl, and IBF was eluted with 0.5 M KCl in buffer A. For columns containing the palindrome (PAL) sequence AGCTTTGCGCATGCGCAA, the sample was loaded in 0.5 M KCl, and IBF was eluted with 1.2 M KCl in buffer A.

IBF from HeLa cells was purified by chromatography of nuclear extracts through oligomerized PAL-Sepharose as described for the IBF of HD3.

For glycosylation assays, the DNA affinity-purified proteins were fractionated by chromatography through succinylated WGA-Sepharose (Vector Laboratories).

Proteins were analyzed by sodium dodecyl sulfate–7.5% polyacrylamide gel electrophoresis (SDS–7.5% PAGE) and stained with silver (57). The protein concentration of purified IBR and IBF was estimated in stained gels or Western immunoblots by comparison to recombinant IBR (rIBR) standards. The protein concentration of extracts and rIBR was determined with the Micro BCA reagent (Pierce).

**IBR sequencing and peptide mapping.** Purified IBR (26 μg) was precipitated with 10 volumes of acetone-acetic acid-triethylamine (90:5:5). The protein was cleaved with CNBr and trypsin, and several peptides separated by high-pressure liquid chromatography (HPLC) were sequenced (W. M. Keck Foundation, Yale University). The sequences obtained were: KRPHVFESNPSIR, VFGAAPLEN VVR, ESCKPIXWPXDIPXANVR, and VSWTQALR.

Purified IBR, IBF, and rIBR in 20 μl of 1% SDS were reacted with 60 μl of 1.3-mg/ml 2-(2′-nitrophenylsulfenyl)-3-methyl-3′-bromoindolenine (BNPS-skatole; Pierce) in acetic acid for 60 min at 47°C, conditions which are specific for cleavage at tryptophan residues (16). The resulting peptides were separated by SDS–14% PAGE and visualized by Western blotting with anti-rIBR antibodies.

**Construction of cDNA libraries and cloning of IBR cDNA.** Double-stranded cDNA was synthesized from immature hen erythrocyte or HD3 polyadenylated [poly(A)$^+$] RNA (67). A partial hen erythrocyte cDNA library was constructed with λZap II (Stratagene), and double-stranded cDNA was fractionated by size by low-melting-point agarose electrophoresis (15). The nonamplified library was screened with a partial IBR cDNA clone obtained by PCR amplification of erythrocyte double-stranded cDNA with the sense primer GGAATTCC(A/C/G)CCNCACGTNTT(C/T)GA and the reverse primer GCTCTAGAGC(C/A)A(G/A)TGC(T/C)TG(G/T/A)GTCCA, corresponding to peptides PVHFE and WTQAL, respectively. PCR conditions were as described before (15). Two IBR cDNA clones were isolated, pcIBR1 and pcIBR2 (Fig. 2), that contained incomplete open reading frames (ORFs) (pcIBR1 encompassing nucleotides 281 to 1691, and pcIBR2 encompassing 738 to 2029). The missing 5′ sequences were obtained by ligation-mediated PCR (LMPCR) (59) with the reverse primers pr1 (GCTCTTGTACTTGCGTACC), pr2 (TACCACATTCTCCAAGGGTGCAG CTC), and pr3 (GAAGACAGGGTTGGGTTTGGAGGGTGA) and the forward linker primer (GCGGTGACCCGGGAGATCTGAATTC). Double-stranded cDNA from immature hen erythrocyte or HD3 cells was denatured, annealed to pr1, elongated with T7 DNA polymerase, and ligated to the common linker. Elongated products were amplified with *Taq* polymerase, using 10 pmol each of pr2 and forward linker primer. The PCR conditions were 1 min at 94°C, 2 min at 63°C, and 3 min at 76°C for 25 cycles in a Perkin Elmer/Cetus DNA thermal cycler. One-hundredth of the reaction was reamplified with pr3 and the forward linker primer (PCR conditions were as above except that the annealing temperature was 67°C). The IBR cDNA- (pcIBR3) and IBF cDNA-specific products were purified by gel electrophoresis and cloned in pCR-1000 (Invitrogen).

A cDNA containing the complete ORF of IBR was reconstructed by swapping the appropriate 5′ and 3′ regions of pcIBR1 and pcIBR3 at a unique *Mlu*I site of the overlapping sequences. The reconstructed plasmid is hereafter referred to as pcIBR. Dideoxy nucleotide sequencing of the two DNA strands was carried out with a T7 DNA polymerase kit (Pharmacia). Band ambiguities were resolved by substituting dGTP with 7-deaza-dGTP or by posttreatment of the elongated products with terminal deoxynucleotidyl transferase (42). Computer DNA and protein sequence analyses were performed with the Genetics Computer Group software.

**Recombinant proteins.** IBR and several deletion mutants were expressed in *Escherichia coli* BL21(DE3) (79) with the vector pET15b (Novagen), as suggested by the manufacturer. For the full-length recombinant protein, rIBR, the parental pcIBR was modified to introduce a FLAG epitope (6) at the N terminus of IBR and a simian virus 40 (SV40) T antigen epitope, recognized by monoclonal antibody kt3 (49), at the C terminus of IBR. This was achieved by PCR of 40 ng of pcIBR with the forward (CGGGATCCCGCCATGGACTACAAGG ACGATGAAGAACACGGCGTGAC) and reverse (CGGGATCCTCATGTT TCTGGTTCTGGTGGAGGTGTCTGTTCCAAAGTTACCAC) primers. The forward primer provided a *Bam*HI site followed by a consensus translation initiation sequence (44) and coded for the additional peptide MDTKDD that was fused to the Glu at position 2 of the IBR reading frame. The reverse primer deleted the natural termination codon of IBR mRNA and added the sequence TPPPEPET, followed by a termination codon and a *Bam*HI site. The amplification conditions were 1 min at 94°C, 1.5 min at 55°C, and 1 min at 72°C for 7 cycles, followed by 1 min at 94°C, 1.5 min at 65°C, and 1 min at 72°C for an additional 18 cycles. The PCR product was digested with *Bam*HI and cloned in pBluescript (Stratagene). This plasmid is referred to as pcIBRFT. DNA sequencing indicated that pcIBRFT contained a T → A transversion at position 333, producing an F → I mutation. To regenerate the wild-type sequence, the fragment *Sph*I-*Mlu*I (155 to 369) of the PCR product was replaced by the same fragment of pcIBR. The cDNA insert of pcIBRFT was digested with *Bam*HI and cloned at the *Bam*HI site of pET15b.

To construct N-terminal deletion mutants of rIBR, the insert of pcIBRFT was cleaved with *Ava*I (ΔN49), *Mlu*I (ΔN110), *Bst*XI (ΔN127), and *Hae*II (ΔN172). Mutant ΔN79 was constructed from pcIBR1. The corresponding cDNA fragments were inserted in a pET15b vector appropriately modified to permit in-frame fusions of the different mutants to the tag of six His residues ($His_6$) provided by the vector.

To construct C-terminal deletion mutants, the pcIBRFT insert was digested with *Ear*I (ΔC424), *Bsa*HI (ΔC333), *Ban*I (ΔC300), *Sau*3aI (ΔC283), and *Fsp*I (ΔC247). The corresponding cDNA fragments were inserted at the *Bam*HI site of a modified pET15b vector that provided termination codons in the three reading frames, immediately downstream of the insertion site.

The recombinant proteins were extracted under nondenaturing conditions as recommended by the manufacturer. rIBR and the C-terminal deletion mutants were purified by heparin-agarose chromatography because translation started at the AUG of cIBRFT rather than at the vector AUG, resulting in proteins that did not contain the $His_6$ tag. N-terminal deletion mutants were purified by affinity chromatography on $Ni^{2+}$-nitrilotriacetic acid-agarose (Qiagen).

pRC/RSV (Invitrogen) was used to construct eukaryotic expression vectors of IBR. DNAs coding for full-size rIBR or N-terminally and C-terminally truncated proteins were excised from the pET15b constructs and inserted at the *Hin*dIII site of pRC/RSV by blunt-end ligation.

All constructs were verified by DNA sequencing.

**Determination of the optimal IBR recognition sequence.** Affinity-purified IBR (100 ng) was incubated with 1 μg of the double-stranded oligonucleotide mixture CGTTGAATTCCGTAGG$(N)_{24}$CAGGCTGAATTCGCAC (i.e., 30-fold molar excess of probe) in 100 μl of binding buffer (100 mM KCl, 20 mM HEPES [pH 7.9], 3 mM $MgCl_2$, 0.1% Nonidet P-40, 1 mM dithiothreitol [DTT], 1 μg of bovine serum albumin per ml, 10% glycerol). After 3 h at 4°C, sonicated salmon sperm DNA was added to a final concentration of 10 μg/ml, and the mixture was loaded on a 100-μl WGA-Sepharose column equilibrated with binding buffer containing salmon sperm DNA. The flowthrough fraction was discarded, and the column was successively washed with 10 volumes of binding buffer, 0.2 M KCl-containing binding buffer, and binding buffer. Oligonucleotide-protein complexes were eluted with 0.3 M *N*-acetylglucosamine in binding buffer, and DNA was purified by phenol extraction. One-fifteenth of the DNA was amplified by PCR in a reaction containing 20 mM Tris (pH 8.3), 50 mM KCl, 2.5 mM $MgCl_2$, 0.01% gelatin, 50 μM each of the four deoxynucleoside triphosphates, 5 U of *Taq* DNA polymerase, and 200 pmol each of forward (CGTTGAATTCCGTAGG) and reverse (GTGCGAATTCAGCCTG) primers. The PCR conditions were 92°C for 1 min, 43°C for 2 min, and 72°C for 0.5 min for 19 cycles. Then 300 ng of amplified probe was incubated with 100 ng of cIBR as indicated above, and the procedure was repeated five or eight times. Oligonucleotides selected by IBR were digested with *Eco*RI (sites underlined in the original sequence) and inserted at the *Eco*RI site of pUC12N23, which contains an $(N)_{23}$ signature sequence at the *Xba*I site of pUC12 to permit identification of independent recombinants.

**Cross-linking.** Purified IBR or partially purified IBF (50 to 60 ng in a 25-μl reaction) were incubated with increasing concentrations of glutaraldehyde (0 to 0.1%) in 25 mM HEPES (pH 7.5)–0.1 M KCl–1 mM EDTA–5 mM $MgCl_2$–8% glycerol for 30 min at 30°C. The reaction was quenched with Tris-HCl (pH 7.5) to a final concentration of 50 mM. Insulin (10 μg) was added as the carrier, and proteins were precipitated and analyzed by Western blot with anti-rIBR antibodies.

**DNA-binding assays and kinetic measurements.** DNase I footprinting and gel retardation assays were carried out as described before (25, 72). Where indicated, the nuclear extracts were incubated with immunoglobulin G (IgG) from preimmune or immune anti-IBR serum for 2 h at room temperature prior to incubation with the labeled oligonucleotide probes. The wild-type and mutant oligonucleotides corresponding to sequences from −20 to +14 and −10 to +14 of the *h5* gene have been described (25). Additional oligonucleotides were PAL (GTAGACTGCGCATGCGCATCT) and 1/2 PAL (GATGTAGACTGCGCAT CTGTATGC).

On-rate determinations were carried out at 0°C with a probe concentration of $6 \times 10^{-9}$ M and purified IBR at $1.2 \times 10^{-9}$ M. Aliquots were loaded at different times in a 4% polyacrylamide gel running at 20 V/cm, and it took 3 min for the DNA complex to enter the gel. For off-rate measurements, the reaction mixtures

were incubated to virtual equilibrium for up to 4 h at 0°C, at which time a 100-fold molar excess of nonlabeled probe was added. Incubation was continued for 0, 1, 3, 5, 10, 20, 40, 60, 105, and 135 min (in the case of the *h5* probe) or for 0, 2, 5, 10, 20, 40, 60, 90, 120, 180, 360, 480, 570, and 720 min (in the case of the PAL probe) before immediately loading the reaction mixtures in a gel. To determine the dissociation constant of the IBR dimers, increasing concentrations of the protein ($0.72 \times 10^{-9}$ to $7.2 \times 10^{-9}$ M) were incubated in the binding buffer for 30 min at 30°C prior to addition of the $^{32}$P-labeled DNA probe ($7.2 \times 10^{-8}$ M), and incubation was continued for an additional 30 min. Gels were fixed for 90 min with 40% methanol–10% acetic acid and dried. The radioactivity of bound and free probes was quantified with a PhosphorImager 445SI (Molecular Dynamics).

**Cells and transfection.** Chicken erythroid HD3 cells [*ts*34 AEV-transformed CFU(E)] and H32 cells (transformed quail fibroblasts) were grown as previously described (72, 73). HD3 cells were induced to differentiate at 41°C with 15 μM H7 (Sigma). H32 cells were transfected with 1 μg of the Rous sarcoma virus (RSV)-IBR expression vectors with Lipofectamine (GIBCO-BRL) as recommended by the manufacturer. Cells were processed at 48 h posttransfection for indirect immunofluorescence assays.

**Antibodies.** Antibodies against affinity DNA-purified chicken IBR were elicited in rabbits injected with a mixture of 1 ml of phosphate-buffered saline (PBS) containing 20 μg of affinity-purified protein and 200 μg of insulin with 0.5 ml of Inject Alum (Pierce). Rabbits were boosted after 3 weeks with the same mixture, and IgG was purified from antisera by protein A-Sepharose chromatography. Antibody reaction was not noticeably affected by periodate oxidation of cIBR, indicating that the antibodies were not specific for carbohydrate epitopes (92).

Rabbit anti-rIBR antibodies were obtained by injection of untagged ΔN79-IBR and purified by affinity chromatography. Monoclonal antibody kt3, specific for the carboxyl terminus of SV40 T antigen (49), was the generous gift of J. Landry.

Indirect immunofluorescence and confocal microscopy were done as described before (15) with anti-rIBR or kt3 as the primary antibody. Texas red-conjugated anti-rabbit Ig or fluorescein-conjugated anti-mouse Ig antibodies were used as secondary reagents.

**IBR phosphorylation.** Purified immature erythrocytes (64) from the peripheral blood of anemic hens were resuspended in 2 ml ($10^8$ cells per ml) of phosphate-free Dulbecco's modified Eagle's medium (GIBCO-BRL) supplemented with dialyzed 8% fetal calf serum and 2% chicken serum and labelled with 2.5 mCi of carrier-free $^{32}P_i$ (New England Nuclear [NEN]) per ml for 17 h at 37°C and 5% $CO_2$. Cells were washed and lysed with 1 ml of buffer B (20 mM HEPES [pH 7.9], 0.5% Nonidet P-40, 0.5% Tween 20, 0.10 M NaCl, 40 mM NaF, 1.5 mM β-naphthylphosphate, 10 mM β-glycerophosphate, 1 mM DTT, 0.4 mM PMSF, 1 mM benzamidine, 1 μM leupeptin, and 1 μM pepstatin). After centrifugation, the crude nuclear pellet was suspended in 100 μl of buffer B supplemented with 0.5% deoxycholate and 1% SDS and boiled for 5 min. The lysate was diluted with 900 μl of buffer B supplemented with 0.2 mM EDTA and 0.2 mM EGTA and centrifuged for 1 h at 40,000 rpm in an SW50.1 rotor. The supernatant was precleared by incubation with 40 μl of neutral rabbit IgG cross-linked (78) to protein A-Sepharose for 18 h at 4°C and reacted with 10 μl of affinity-purified anti-rIBR IgG cross-linked to protein A-Sepharose for an additional 18 h at 4°C. The beads were washed four times with 0.1% SDS containing buffer B, resuspended in 1 volume of 2× electrophoresis sample buffer, and boiled for 3 min before loading the gel. Proteins separated by electrophoresis were transferred onto a 0.2-μm nitrocellulose membrane (Schleicher and Schüll). After $^{32}$P detection by autoradiography, the membrane was reacted with anti-rIBR antibodies.

For CK-II assays, 500 ng of rIBR or ΔN79-IBR in 10 μl of 20 mM HEPES (pH 7.4)–0.1 M NaCl–10 mM $MgCl_2$–60 μM ATP–1 μM leupeptin–1 μM pepstatin, 0.4 mM PMSF containing 5 μCi of [γ-$^{32}$P]ATP (3,000 Ci/mmol; NEN) was treated with 10 ng of CK-II (Kinetek Biotechnology Corp.) for 30 min at 30°C. Reactions were terminated by addition of electrophoresis sample buffer and boiling for 2 min. CK-II was omitted from control reactions.

For $p42^{MAPK}$ kinase (ERK2) assays, CCL39 hamster fibroblasts were mock transfected or transfected with pEXV-ERK2-Tag, a vector expressing mouse ERK2 tagged with a c-Myc epitope recognized by monoclonal antibody 9E10 (34). At 60 h posttransfection, cells were deprived of serum for 24 h and induced or not with 1% fetal calf serum for 10 min. Cell extracts were immediately prepared in buffer D (20 mM Tris [pH 7.5], 0.15 M NaCl, 0.1 mM EDTA, 1 mM EGTA, 1 mM $MgCl_2$, 1 mM sodium vanadate, 1% Triton X-100, 1 mM PMSF, and 1 μM leupeptin) and reacted with antibody 9E10 bound to protein A-Sepharose. Then 2 μg of rIBR or myelin basic protein was mixed with aliquots of the immunoprecipitates in a 30-μl reaction for 25 min at 30°C. The reaction cocktail contained 1.5 μCi of [γ-$^{32}$P]ATP, 25 μM ATP, 15 mM MOPS (morpholinepropanesulfonic acid, pH 7.0), 5% glycerol, 60 mM *para*-nitrophenyl phosphate, 15 mM $MgCl_2$, 1 mM DTT, 1 μM leupeptin, 0.1 mM PMSF, and 0.3 μg of cyclic AMP (cAMP)-dependent protein kinase inhibitor (Sigma). Reactions were quenched by addition of electrophoresis sample buffer and boiling for 2 min.

**Blot analyses.** Western blot analyses were done as described before (74) except that chemiluminescence was used for detection (ECL; Amersham). For Northern (RNA blot) analysis, total RNA from undifferentiated and differentiated HD3 cells and poly(A)$^+$ RNA from immature hen erythrocytes were separated by electrophoresis in formaldehyde-agarose gels and transferred to a Hybond-N membrane (Amersham). For Southern analysis, restriction nuclease-digested erythrocyte DNA was separated by electrophoresis in 0.5% agarose gels and transferred to a Hybond-N membrane. Blotted nucleic acids were hybridized with the insert of pcIBR1 labeled by random priming with a DNA labeling kit (Pharmacia). The sizes of proteins, RNA, or DNA were estimated from those of appropriate standards run in parallel lanes.

## RESULTS

**IBR and IBF are related proteins.** Gel retardation assays indicated that HeLa cells contain a nuclear protein which formed a specific complex with a probe containing the transcription initiation site of the histone *h5* gene. The electrophoretic mobility of the complex was identical to that formed by IBR from chicken erythrocytes and IBF from HD3 (Fig. 1A, IBR/IBF). An additional complex made by the HeLa nuclear extract (Fig. 1A, band X) was nonspecific, since its formation was prevented by competition with an oligonucleotide containing a mutated IBR/IBF binding site (Fig. 1A). Similar assays with nuclear proteins from chicken brain and T lymphoblastoma cells (MSB-1), transformed H32 quail fibroblasts, mouse L cells, and rat liver (not shown) further indicated that all the systems studied contained a DNA-binding protein related to IBR or IBF. Therefore, IBR or IBF appears to be ubiquitous.

To investigate the relationship among these specific DNA-binding proteins, the erythrocyte, HD3, and HeLa extracts were incubated with purified rabbit anti-IBR IgG prior to incubation with the *h5* probe. Pretreatment with the antibodies reduced the amount of the specific complexes in a concentration-dependent manner (Fig. 1B). At the lower antibody dosage, a supershifted complex was clearly observed for each of the extracts (Fig. 1B, SS), the amount of which was related to the concentration of the specific DNA-binding protein of the extract. At higher antibody dosages, the complexes were probably immunoprecipitated and did not enter the gel. On the other hand, preincubation of the extracts with preimmune IgG did not affect the mobility of the specific complexes (Fig. 1B). Figure 1C shows that the anti-IBR IgG also recognized the proteins from the three nuclear extracts after purification by affinity chromatography with the oligomerized *h5* oligonucleotide. IBR from erythrocytes showed a slower electrophoretic mobility (70 to 73 kDa) than IBF from HD3 (68 to 70 kDa) (Fig. 1C, lanes 1 and 2), in accordance with our previous results (25), whereas the HeLa protein had the same mobility as IBF, although the relative proportion of the 70-kDa species was higher (Fig. 1C, lane 3). Although the heterogeneity of the proteins could reflect their posttranslational modifications (see below), the 68-kDa component appears to be a proteolytic product of the 70-kDa species, since its relative proportion varied from preparation to preparation and increased with handling of the sample (Fig. 1C, cf. lanes 4 and 5).

In conclusion, these results indicate that IBR is structurally related to IBF (HD3) and that HeLa cells contain a protein which is probably the human homolog of IBF.

**Cloning and analysis of IBR cDNA.** To characterize IBR and to determine its structural relationship with IBF, we undertook the cloning of IBR cDNA. Purified IBR from mature erythrocytes was cleaved with CNBr and trypsin, and four peptides separated by HPLC were sequenced (Fig. 2). A computer-assisted search of the GenBank and SwissProt databases revealed that P3A2, a transcription factor isolated from sea urchin embryos (11), contained almost identical sequences. To obtain a probe for IBR cDNA cloning, double-stranded cDNA from immature erythrocytes was amplified by PCR with degenerate oligonucleotide primers corresponding to the outer PHVFE and WTQAL peptides of IBR according to the P3A2

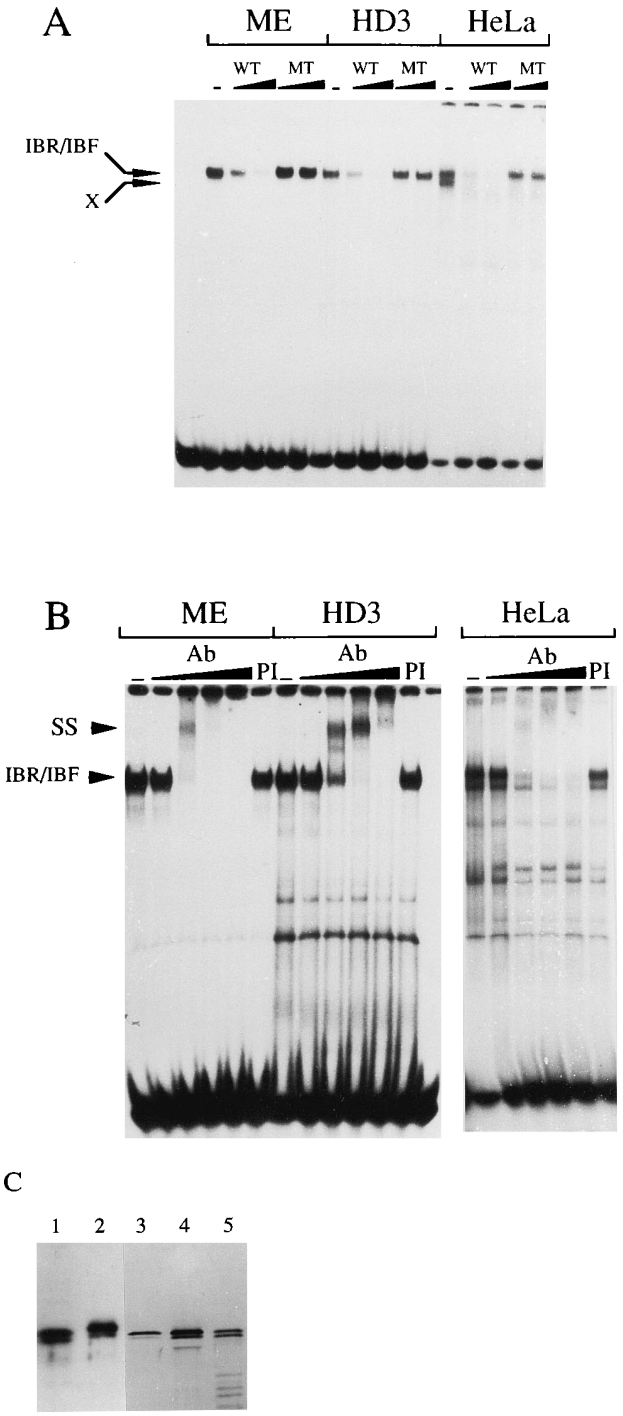


FIG. 1. Specific binding of IBR from mature erythrocytes (ME) and IBF from HD3 and HeLa cells to the transcription initiation region of the *h5* gene. (A) Gel retardation assays of a $^{32}$P-labeled *h5* probe (−20 to +14) incubated with the indicated nuclear extracts. Leftmost lane, no protein; lanes —, no competitor oligonucleotide; lanes WT and MT, competition with a 20-fold and 80-fold molar excess of nonlabeled wild-type or mutant oligonucleotide probe, respectively. (B) Antibodies against IBR recognize the specific *h5*-binding factors of HD3 and HeLa. Gel retardation assays of the *h5* probe incubated with the indicated nuclear extracts pretreated with anti-IBR IgG. Lanes —, no antibody; lanes Ab, preincubation for 2 h with 50, 125, and 250 μg of anti-IBR IgG; lanes PI, preincubation for 2 h with 250 μg of preimmune IgG; last lane of the HD3 set, free probe. The specific IBR/F and supershifted (SS) complexes are indicated. (C) Antibodies against IBR recognize IBF. IBR from mature erythrocytes and IBF from HD3 and HeLa cells were purified and analyzed by Western blot with anti-IBR antibodies. Lanes 1, 4, and 5, IBF (HD3); lane 2, IBR; lane 3, IBF (HeLa).

sequence. The sequence of the amplified DNA product encompassed a reading frame coding for the two internal peptides, while the rest of the sequence confirmed the strong homology of IBR with P3A2. Moreover, the erythrocyte PCR product and a 456-bp PCR product of chicken liver cDNA amplified with different P3A2-specific primers (kindly provided by F. Calzone) had identical overlapping sequences. This result further indicated that IBR is the chicken homolog of P3A2.

Since the size of IBR mRNA was estimated to be $3.6 \times 10^3$ nucleotides (see Fig. 5A), a partial cDNA library was constructed with size-fractionated double-stranded cDNA of >1.5 kbp to enrich the IBR cDNA. Screening of $6 \times 10^5$ recombinant phages of the nonamplified library with the PCR probe resulted in the isolation of two overlapping IBR cDNA clones, pcIBR1 and pcIBR2 (Fig. 2), which contained incomplete ORFs (i.e., without the initiator methionine) and different lengths of 3′ untranslated (UTR) sequences. Because further screening of the library yielded no additional positive clones, the missing 5′ sequences were obtained by LMPCR of erythrocyte cDNA with nested reverse primers located downstream of the unique *Mlu*I site of pcIBR1. The major amplified DNA product (pcIBR3 [Fig. 2]) contained the expected pcIBR1 overlapping fragment and additional 5′ sequences that included a putative initiator ATG. Although the sequences upstream of the AUG codon could code for additional N-terminal amino acids, we considered this unlikely because no PCR products longer than pcIBR3 were detected by hybridization with pcIBR1. Therefore, a cDNA containing the complete ORF of IBR, referred to as pcIBR, was constructed by swapping the 5′ fragment of pcIBR3 and the 3′ fragment of pcIBR1 at the unique *Mlu*I site (Fig. 2). Although pcIBR2 ends with a stretch of poly(A), this sequence is likely to represent not the true 3′ end of the mRNA but the product of internal oligo(dT) priming at this tract, since erythrocyte IBR mRNA is 3.6 kb long (see Fig. 5A). Consistent with this interpretation, Southern blot analysis of the erythrocyte double-stranded cDNA indicated the presence of a major species (>95%) of about 2 kbp (not shown). Therefore, we concluded that approximately 1.6 kb of 3′ UTR were missing from the cloned cDNA.

The sequence of pcIBR predicts an acidic protein ($pK_a$ = 4.8) of 503 amino acids (53.6 kDa) with strong local homology to P3A2 (see below). The calculated mass of IBR is 27% smaller than that estimated by SDS-PAGE. This discrepancy is mainly due to an anomalous electrophoretic behavior of the protein, as already noted for P3A2 (11) and other related factors (see below), since the recombinant protein (rIBR) made in *E. coli* had an electrophoretic mobility similar to that of natural IBR (see Fig. 8A).

Figure 2 also shows a schematic map of IBR based on its amino acid composition, the DNA-binding/dimerization domain, several putative CK-II sites, and the NLS (see below). The 36 N-terminal residues, relatively glutamine-rich (14%), are followed by an acidic region ($pK_a$ = 2.9), comprising residues 37 to 67, that contains several putative sites for CK-II, at least one of which is phosphorylated in vitro by the purified kinase (see Fig. 8B). This region is separated by an alanine-rich (48%) motif, encompassing residues 68 to 88, from a basic segment, residues 89 to 127 ($pK_a$ = 12.3), which harbors a putative bipartite NLS (see Fig. 13). The region from residues 127 to 285 is neutral and relatively proline-rich, whereas the rest of the molecule is acidic ($pK_a$ = 3.6) and relatively glutamine-rich.

**DNA-binding specificity of recombinant IBR.** To ascertain that IBR and rIBR recognized identical DNA sequences, their footprints on the *h5* promoter were analyzed. The *h5* gene

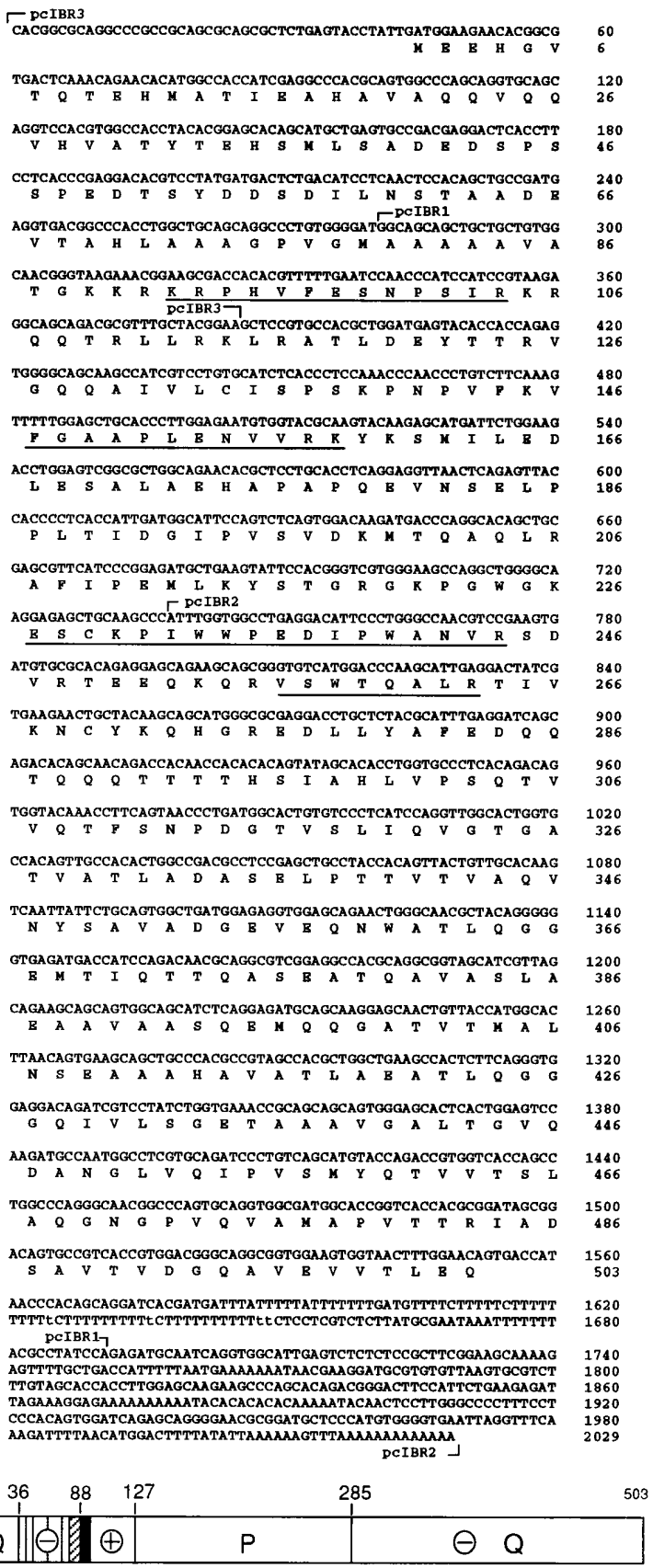
pcIBR3
pcIBR1
pcIBR3
pcIBR2
pcIBR1
pcIBR2
36
88
127
285
503
Q
P
Q

FIG. 2. Nucleotide sequence of a partial IBR cDNA (pcIBR; EMBL database accession number X86013) and deduced protein sequence of IBR. pcIBR was reconstructed from the cDNA clones pcIBR1 to pcIBR3, as indicated. Nucleotides present in pcIBR1 and not in pcIBR2 are shown in lowercase letters. Underscored amino acids correspond to the peptide sequences determined from purified IBR. A schematic representation of IBR subregions is given below the sequence. Q, glutamine-rich regions (12 to 14%); P, proline-rich region (9%); −, acidic regions ($pK_a$, 2.9 to 3.6); +, a highly basic region ($pK_a$, 12.3). Vertical broken lines correspond to putative CK-II sites. The solid box shows the bipartite nuclear localization signal, and the hatched box shows an alanine-rich region (48%).

contains several IBR/IBF binding motifs, including a series of 6-bp overlapping sites (Fig. 3B, boxes B to E), the −7 to +5 site (box C) having the highest affinity and strongest methylation interference (25). The DNase I assays (Fig. 3A) indicated that rIBR protected the same regions as IBR and IBF, including sequences upstream and downstream of the *h5* transcription initiation site. At the lower protein concentrations, the three proteins first protected sites B to E, followed by the half-site A. At the higher rIBR concentration used, a protection of the lowest-affinity site F was also observed. The additional footprint upstream of A, observed with the three proteins, corresponds to an *Fsp*I site of the pBR322 vector that has the sequence TGCGCA, corresponding to half of the IBR optimal recognition site (see below). These results, together with the ability of IBR and rIBR to form complexes with *h5* probes that have the same electrophoretic mobility (not shown), further indicated that pcIBR encodes bona fide IBR.

**Homology of IBR to related nuclear factors.** During the course of this work, the sequences of two proteins highly related to IBR, *Drosophila* EWG (17), and human NRF-1 (88), became available. EWG is involved in the development of the central nervous system and flight muscles. Although the DNA-binding and transcriptional effects of EWG were not investigated, this protein is likely to be a transcription factor by analogy to the other proteins of this family. NRF-1 is a transcriptional activator of nuclear genes involved in mitochondrial energy transduction (88) and is identical to the recently reported human α-Pal factor (18), which activates transcription of the gene (*eif-2α*) coding for the α subunit of the translation initiation factor IF-2. In common with IBR and P3A2, these proteins behaved in SDS-PAGE as having apparent molecular masses 30 to 50% larger than those predicted from their respective cDNAs.

A comparison of the structurally related factors showed that IBR has the same size as and 99% overall identity with NRF-1/α-Pal (Fig. 4), clearly indicating that it is the chicken homolog of the human factor. The five changes between the sequences of IBR and NRF-1/α-Pal occur in the C-terminal half of the proteins at residues 289 (Q→T), 291 (T→A), 293 (T→A), 485 (A→S), and 491 (V→M). The homology between

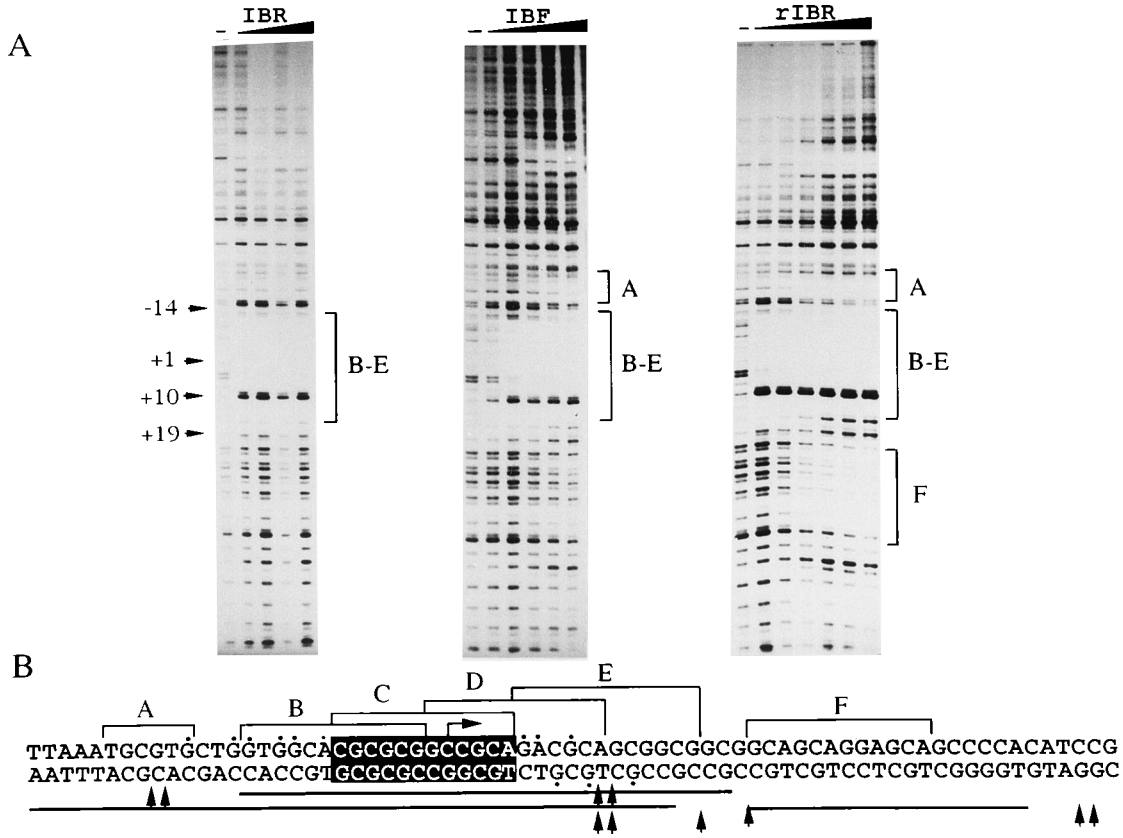


FIG. 3. Footprint of IBR, IBF, and rIBR on the transcription initiation region of the *h5* gene. (A) A $^{32}P$-labeled probe of the *h5* gene (−388 to +72) was incubated with increasing concentrations of the purified proteins before digestion with DNase I: IBR, 7, 10, 15, and 20 ng; IBF, 3, 6, 12, 25, and 50 ng; and rIBR, 4, 8, 16, 32, 64, and 128 ng. Lanes —, no protein. The position of the footprints was determined from G+A sequence ladders run in parallel lanes. (B) Summary of the footprints at moderate and higher concentrations of protein (upper and lower lines underneath the sequence, respectively) and DNase I-hypersensitive sites (arrowheads). The solid box and the dots indicate nucleotides showing maximal and partial methylation interference (25). The 6-bp-overlapping 12-bp IBR/F binding sites (A to F) are marked by brackets. The bent arrow indicates the major *h5* transcription initiation site (+1).

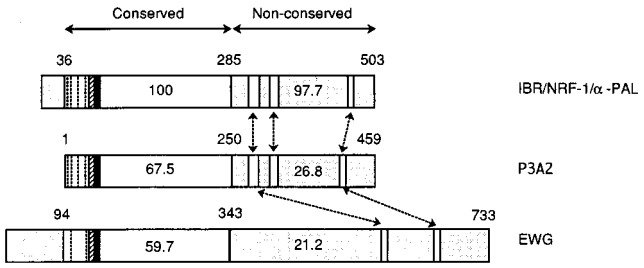


FIG. 4. Homology of IBR to related transcription factors. The sequences compared with IBR are NRF-1/α-Pal (18, 88), sea urchin P3A2 (11), and *Drosophila* EWG (17). The percentage of amino acid identity between the evolutionarily conserved and nonconserved regions is indicated inside the boxes. Patches of homology in the C-terminal halves are indicated by the open boxes. Other symbols are as in Fig. 2.

the vertebrate and invertebrate factors is only segmental, EWG having longer N- and C-terminal sequences, whereas P3A2 has a shorter N-terminal sequence. However, residues 36 to 285 of IBR have been evolutionarily conserved with respect to residues 1 to 250 of P3A2 (67.5% identity) and residues 94 to 343 of EWG (59.7% identity). Interestingly, these regions encompass the DNA-binding and dimerization domains, as well as the NLS and some of the potential CK-II sites (see below, Fig. 8, 12, and 13). On the other hand, the C-terminal halves have low general sequence conservation (26.8% and 21.2% identity for P3A2 and EWG, respectively), although they have patches of significant homology (i.e., IBR 312 to 334 with P3A2 285 to 302 and EWG 552 to 562, IBR 377 to 392 and P3A2 339 to 354, IBR 454 to 464 with P3A2 396 to 406 and EWG 639 to 649 [Fig. 4]).

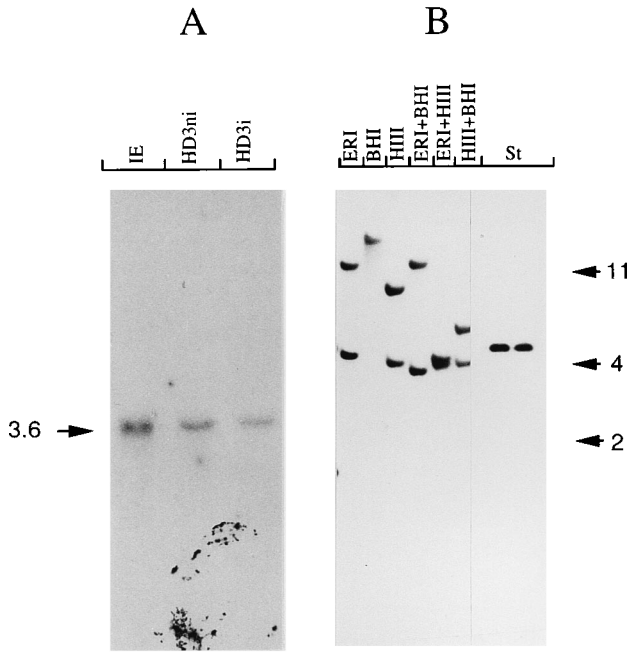


FIG. 5. (A) Northern and (B) Southern blot analyses of nucleic acids from chicken erythroid cells hybridized with $^{32}$P-labeled pcIBR1. (A) Lanes HD3ni and HD3i, 16 and 20 μg of total RNA from nondifferentiated and differentiated HD3 cells, respectively; lane IE, 4 μg of poly(A)$^+$ RNA from immature adult erythrocytes. (B) Hen erythrocyte DNA (10 μg) was digested with *Eco*RI (ERI), *Bam*HI (BHI), *Hin*dIII (HIII), or a combination of them. Lanes St contained an amount of pcIBR1 DNA equivalent to one copy per haploid chicken genome. The sizes of the fragments (in kilobases) were estimated from RNA and DNA markers run in parallel lanes.

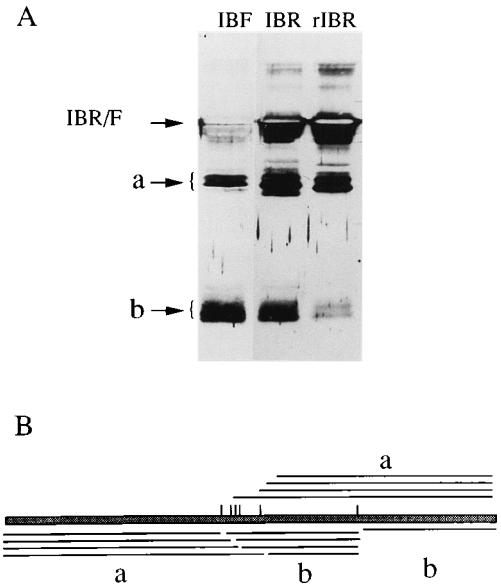


FIG. 6. Peptide maps of IBR, IBF, and rIBR. (A) The purified proteins were partially cleaved at tryptophan residues with BNPS-skatole, and the products were analyzed by Western blot with anti-rIBR antibodies. (B) Summary of the positions of tryptophan residues in IBR and the origin of the cleaved peptides.

**IBR and IBF are the products of the same gene.** RNA from immature erythrocytes and undifferentiated or differentiated HD3 cells revealed the presence of a unique species of about 3.6 kb when hybridized to a pcIBR1 probe (Fig. 5A). Amplification by LMPCR of double-stranded cDNA from immature erythrocyte and HD3 cells with specific IBR cDNA primers yielded fragments similar in length and identical in DNA sequence (not shown). These results, together with the other properties common to IBR and IBF, such as epitopes, DNA-binding specificity, footprints, and mobility of the DNA complexes, suggested that the two proteins are probably coded by the same gene. Southern analysis of genomic chicken DNA hybridized with pcIBR1 indicated that the *ibr* gene is unique (Fig. 5B), and hybridization under less stringent conditions failed to detect other genomic DNA fragments having about 80% identity to the probe (not shown). These results further supported the view that IBR and IBF have the same sequence, although the possibility that IBR and IBF were the products of alternative splicing was not ruled out. To examine this, purified IBR, IBF, and rIBR were reacted with BNPS-skatole, a reagent that specifically cleaves at tryptophan residues (16), and the products of cleavage were analyzed by Western blot. Figure 6 shows that the affinity-purified anti-rIBR antibody recognized the same partial digestion products of the three proteins, further indicating that IBR and IBF have identical amino acid sequences. Although we cannot completely exclude that IBR and IBF differ by the presence or absence of a short peptide sequence, the almost identical sequences of IBR and NRF-1/α-Pal and the identical electrophoretic mobilities of IBF and NRF-1/α-Pal make this possibility remote.

**IBR and IBF differ in extent of glycosylation.** If IBR and IBF have the same primary structure, it follows that their different electrophoretic behaviors should reflect differential posttranslational modifications. Since previous results have suggested that IBR contains *N*-acetylglucosamine residues (25), we investigated whether IBR and IBF had different degrees of glycosylation. Nuclear extracts from erythrocytes and HD3 cells were fractionated into succinylated WGA-binding and non-

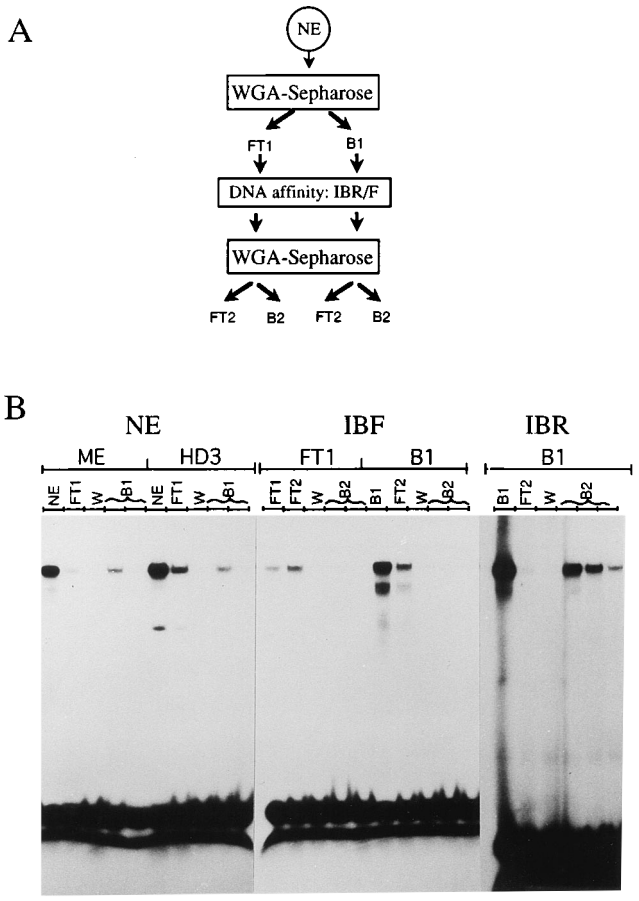


FIG. 7. Glycosylation of IBR. (A) Nuclear extracts (NE) from mature erythrocytes (ME) and HD3 cells were fractionated into WGA-binding (B1) and nonbinding (FT1) proteins. IBR and IBF from each of the fractions were purified by DNA affinity chromatography and separated again into WGA-binding (B2) and nonbinding (FT2) fractions. (B) Gel retardation assays of a $^{32}$P-labeled oligonucleotide probe of the *h5* gene (−20 to +14) incubated with proteins from the fractions described for panel A. Lanes W contained wash fractions between the flowthrough and 0.3 M *N*-acetylglucosamine elution.

binding proteins (Fig. 7A), and the presence of the factors in the various fractions was detected by gel retardation assays with the *h5* probe (Fig. 7B). As expected, IBR from the erythrocyte extract was retained by the WGA column, and it was subsequently eluted with *N*-acetylglucosamine. On the other hand, IBF from the HD3 extract was only partially retained under the same conditions (Fig. 7B). Although this suggested that IBF was partially glycosylated, as reported for other transcription factors that behaved in this way in a similar assay (38), the possibility existed that the proteins were indirectly retained by WGA through specific or nonspecific interactions with other glycosylated proteins. Therefore, IBR and IBF from the WGA-bound and nonbound fractions were purified by DNA affinity chromatography, and their ability to bind WGA as purified proteins was reassessed. Clearly, while purified IBR was quantitatively retained by the second WGA column and was eluted with *N*-acetylglucosamine, IBF was not retained whether or not it belonged to the original WGA-bound or unbound fraction (Fig. 7B). Since the behavior of IBF was not due to the action of deglycosylases that could be present in the extract, as judged from the mobility of IBF in the original extract and purified fraction, the results demonstrated that IBF is either not glycosylated or glycosylated to a much lesser extent than IBR. Other experiments also indicated that IBF from HeLa cells (i.e., NRF-1/α-Pal), rat liver, and chicken brain was not detectably glycosylated, whereas IBR from 5-day embryonic erythrocytes was partially glycosylated. We concluded that IBR is a glycosylated form of IBF and that, within the limits of detection, IBR glycosylation is an erythrocyte-specific modification. Therefore, the differential glycosylation of IBR is probably responsible for its slower electrophoretic mobility, since treatment of purified IBR and IBF with acid or alkaline phosphatases did not change their electrophoretic mobilities (not shown).

**Phosphorylation of IBR/F.** Despite the negative phosphatase results, we determined whether IBR/F is phosphorylated in vivo because phosphorylation mediates a variety of biological responses (36) and details about the responsible kinases may give information on the regulatory pathways in which the factor is involved. Immature erythrocytes were incubated with $^{32}P_i$, and IBR/F was immunoprecipitated from the nuclear extract with affinity-purified anti-rIBR antibodies. Autoradiography of the immunoprecipitated proteins separated by SDS-PAGE and transferred to a nitrocellulose membrane revealed a doublet (Fig. 8A, lane a) corresponding to IBR, as demonstrated by treatment of the same membrane with anti-rIBR antibodies (Fig. 8A, lanes b to d).

A survey of the IBR/F sequence for possible kinase consensus sites indicated that the region extending from 38 to 70 contained a cluster of four CK-II and one mitogen-activated protein (MAP) kinase consensus sites. The clustering of sites and their evolutionary conservation (Fig. 2 and 4) hinted that they could be actual phosphorylation sites. This was tested by incubation of rIBR with purified CK-II in the presence of [γ-$^{32}$P]ATP. Figure 8B shows that rIBR was indeed phosphorylated and that phosphorylation was dependent on the presence of CK-II. On the other hand, the deletion mutant ΔN79,

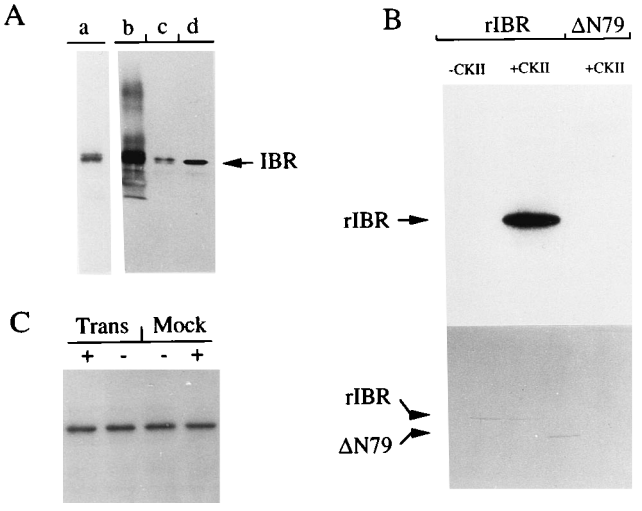


FIG. 8. IBR/F phosphorylation in vivo and in vitro. (A) Immunoprecipitated proteins from immature adult erythrocytes incubated with $^{32}P_i$ were separated by SDS-PAGE and transferred to a nitrocellulose membrane. Lane a, autoradiography; lanes b to d, Western blot with anti-rIBR antibodies. Lane b, same as lane a; lane c, IBR purified from mature erythrocytes; lane d, rIBR. (B) rIBR and the ΔN79 deletion mutant were incubated with [γ-$^{32}$P]ATP in the presence or absence of purified CK-II, as indicated. The upper part of the figure shows an autoradiograph of the proteins separated by SDS-PAGE, and the lower part shows the stained gel. (C) rIBR was incubated with [γ-$^{32}$P]ATP in the presence of immunoprecipitated p42$^{MAPK}$ from quiescent (−) or serum stimulated (+) CCL39 cells transfected (Trans) with an epitope-tagged p42$^{MAPK}$ expression vector or a nonspecific immunoprecipitate from mock-transfected cells (Mock).

lacking the 79 N-terminal amino acids, was not phosphorylated (Fig. 8B). Therefore, at least one of the putative CK-II sites was recognized by the kinase.

Similar experiments were carried out with activated p42 MAP kinase from mitogen-stimulated *p42*$^{MAPK}$-transfected CCL39 cells. The results indicated that this particular MAP kinase was not able to phosphorylate rIBR (Fig. 8C), even though parallel control experiments with myelin basic protein (a substrate of MAP kinases) indicated that p42$^{MAPK}$ was active. The labeling of rIBR that was observed in these experiments was due to a contaminating constitutive protein kinase(s), since it was independent of *p42*$^{MAPK}$ expression or mitogen activation of the cells.

The above results indicate that CK-II is potentially one of the kinases that phosphorylate IBR/F in vivo, but they do not exclude the action of other kinases. Thus, the same N-terminal region contains two CK-I consensus sites, and the DNA-binding/dimerization domain contains a possible p34$^{cdc2}$ and several possible DNA-dependent kinase sites.

**Selection of binding sites from random oligonucleotides.** The finding that IBR is the chicken homolog of human NRF-1/α-Pal was surprising because their DNA recognition sequences appeared to be rather different. In the case of NRF-1, a consensus motif, YGCGCAYGCGCR (where Y is C or T and R is G or A), was derived from comparison of the sequences recognized by the factor in a few promoters (19). In the case of α-Pal, the palindrome TGCGCATGCGCA was derived from a statistical analysis of 67 sequences bound by the factor after only a single cycle of selection with a probe containing randomized $(N)_{14}$ tracts (18). As in the case of NRF-1, the optimal sequence did not differ significantly from that present in the *eif-2*α promoter used to identify the factor. Because the consensus/optimal NRF-1/α-Pal DNA-binding sequences did not readily conform to the *h5* binding sequence (25) (see also Fig. 3), and because a 14-bp randomized stretch could impose constraints on a 12-bp binding factor, we decided to independently determine the optimal sequences recognized by IBR.

A large molar excess of a pool of oligonucleotides containing centrally located $(N)_{24}$ random tracts was incubated with purified IBR, and the complexes were enriched by WGA affinity chromatography, taking advantage of IBR glycosylation (see Fig. 7). After the resin was washed under more stringent salt conditions, the bound complexes were eluted with *N*-acetylglucosamine, and the DNA moiety was amplified by PCR and used in a subsequent selection cycle. Figure 9A shows a summary of 54 independent sequences selected by IBR after five consecutive cycles. The palindromic direct repeat sequence TGCGCATGCGCA, identical to that reported for α-Pal (18), was derived. However, we noticed that the perfect palindrome and half-palindrome sequences represented 1.8 and 66% of the binding sites, respectively, suggesting that the factor could bind modified versions of the palindrome with high affinity. In fact, the central 8-bp palindrome CGCATGCG was present in 54% of the sequences, and this number increased to 81% if allowance was made for one mismatch that conserved the alternating purine-pyrimidine motif of the sequence.

To further test the significance of the palindrome, three supplementary selection cycles were performed, and the sequence of 24 additional binding sites was determined. The results (Fig. 9B) strengthened the statistical significance of the perfect palindrome, the frequency of which increased to 8.3%, but also revealed that the 8-bp palindrome CGCATGCG was present in 83% of the clones. Again, this number raised to 96% if one transition change was allowed in the alternating purine-pyrimidine sequence. We note that despite the AT bias at the dyad of the palindrome, a sequence containing GC at this position was obtained even after eight cycles of selection (Fig. 9B). Hence, although the perfect 12-bp palindrome is probably the highest affinity site for IBR, the more general consensus sequence RCGCRYGCGY is more appropriate as a representative of potential high-affinity sites (see Discussion). IBR might thus recognize structural characteristics of DNA other than sequence, since alternate purine-pyrimidine sequences have the potential to adopt a z-DNA conformation (91).

**A**

| | T | G | C | G | C | A | T | G | C | G | C | A |
|---|---|---|---|---|---|---|---|---|---|---|---|---|
| | 68 | 65 | 95 | 89 | 98 | 95 | 89 | 98 | 87 | 85 | 70 | 67 |
| T | 37 | 0 | 1 | 1 | 1 | 0 | 48 | 0 | 4 | 3 | 13 | 3 |
| C | 7 | 1 | 51 | 1 | 53 | 1 | 5 | 0 | 47 | 1 | 38 | 11 |
| G | 8 | 35 | 0 | 48 | 0 | 2 | 1 | 53 | 1 | 46 | 0 | 4 |
| A | 2 | 18 | 2 | 4 | 0 | 51 | 0 | 1 | 2 | 4 | 3 | 36 |

**B**

cctgTACAATGCGCATGCGCACCTAGAGccta
cctgCGCATGCGTAATACTTCTCGTTACccta
cctgGCCAAGGTTGTGCGCATGCTCATTcctа
cctgCGCATGCGTACATACTTTCCATTGccta
cctgTACCCTTGAATGCGCATGCGCTGTccta
taggGACGGAAGCGCATGCGCGGTGCCCcagg
cctgACAGGAATACGCATGCGCTCTCGAccta
cctgTACACCATTGCGCATGCGTCCGTAccta
cctgGCAAGATGTCAATTCGCGCATGCGcta
taggTACGGAAATGGCGCATGCGTATTGcagg
cctgCGCATGCGTGGTGGTGTTTCCATAccta
cctgATTACACGCAGTATTGCGCATGCGcta
taggTACGGAGCGTGTTATGCGCATGCGagg
taggATAAACAGCGCATGCGCATCAGCCcagg
cctgTAACGACTGGCGCATGCGCATGTTcta
taggTCGGTAGATGTTTTGATGCGCGCGagg
cctgCGCATGCGTGAACCATTCTAACGTcta
taggTACGCATGCGCAGCACTTACTTCGcagg
cctgCACGCATGCGCAGAGGTGTCTCTcta
taggGATACTACGCGTGCGCTGGAACAAcagg
taggCGCATGCGCAATATTATGCGACTAcagg
cctgTGAAACTGAATGCGCATGCGCTAActa
taggTATATGCGCACGCACTCATTCGCcagg
taggCGCATGCGTGGAGTTGCGATAGATcagg

| | T | G | C | G | C | A | T | G | C | G | C | A |
|---|---|---|---|---|---|---|---|---|---|---|---|---|
| | 62 | 79 | 96 | 100 | 100 | 92 | 92 | 100 | 100 | 92 | 71 | 50 |
| T | 15 | 0 | 1 | 0 | 0 | 0 | 22 | 0 | 0 | 1 | 7 | 5 |
| C | 2 | 0 | 23 | 0 | 24 | 0 | 2 | 0 | 24 | 0 | 17 | 3 |
| G | 5 | 19 | 0 | 24 | 0 | 2 | 0 | 24 | 0 | 22 | 0 | 4 |
| A | 2 | 5 | 0 | 0 | 0 | 22 | 0 | 0 | 0 | 1 | 0 | 12 |

FIG. 9. IBR binding site selection. Purified IBR was incubated with a pool of 53-mer oligonucleotides containing random $(N)_{24}$ stretches in the middle of the sequence. Complexes were purified by WGA-Sepharose chromatography, and the oligonucleotide moieties were amplified by PCR and used in a subsequent cycle of selection. (A) Summary of the IBR binding sequences from 54 independent clones after five consecutive cycles of selection. The projected optimal sequence is boxed, and the frequency of each nucleotide is given as a percentage. (B) Sequences of 24 binding sites after eight cycles of selection and sequence summary. Nucleotides in lowercase letters correspond to the constant sequence of the 53-mer flanking the random $(N)_{24}$ tracts.

**IBR and IBF associate as stable homodimers.** The fact that the recognition site of IBR is a palindrome insinuated that the factor binds to DNA as a dimer, in accordance with the Stokes' radius determined by molecular filtration (not shown). On the other hand, because the optimal recognition sequence is also a direct repeat, the possibility that IBR binds to DNA as two independent monomers could not be dismissed. To investigate the type of complex made in solution, IBR and IBF were reacted with increasing concentrations of glutaraldehyde, and the products of the reaction were analyzed by SDS-PAGE and Western blot with affinity-purified anti-rIBR antibodies. Figure 10A shows that the monomer species were cross-linked into dimers, by comparison with the mobility of standard proteins, and that no higher-order oligomers were produced. The higher concentration of glutaraldehyde needed to cross-link IBF was

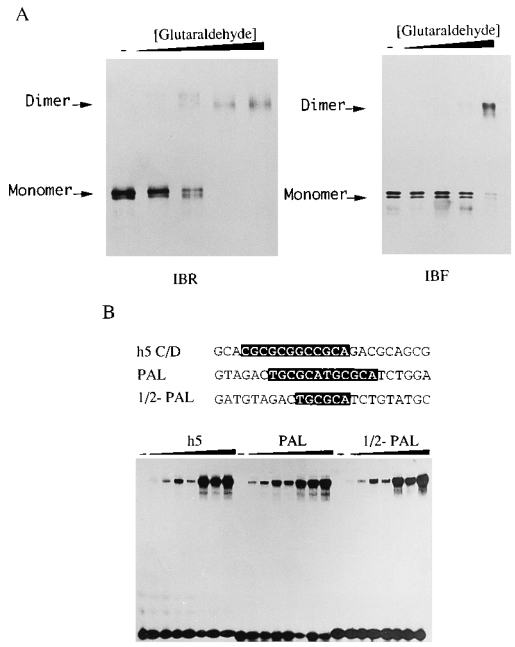


FIG. 10. (A) IBR and IBF associate and bind to DNA as homodimers. Approximately 50 ng of IBR or partially purified IBF was reacted with glutaraldehyde (final concentrations: 0.005, 0.01, 0.025, and 0.1%) for 30 min at 30°C. The products of the reactions were analyzed by Western blot with purified anti-IBR (IBR) or anti-rIBR (IBF) IgG. The apparent molecular masses of the monomer and dimer species were determined by comparison with that of standard proteins run in a parallel lane. (B) Gel retardation assays of $^{32}$P-labeled 24-mer oligonucleotide probes containing either the −10 to +14 sequences of *h5* (*h5*), a perfect palindrome (PAL), or a perfect half palindrome (1/2 PAL), incubated without protein (−) or with 0.5, 1, 2, 0.7, 4, 3, or 6 ng of affinity-purified IBR.

probably related to the presence of other proteins in the partially purified sample. Under the same conditions, the monomeric histone H5 was cross-linked into higher-order oligomers (not shown). Therefore, the homodimer is the main molecular form of IBR and IBF at the concentration of protein used.

We next determined if the dimer was the active DNA-binding species by characterizing the complexes formed by IBR with probes containing the 12-bp palindrome (PAL), the 6-bp half-palindrome (1/2 PAL), and the *h5* sequences. Gel retardation assays indicated that at the IBR concentrations tested, the complexes had identical electrophoretic mobilities (Fig. 10B), implying that IBR recognized the probes as an identical molecular species whether or not the site contained the full or the half recognition sequence. Because no faster-mobility complex could be detected even at the lowest protein concentrations used, it follows that the monomer cannot stably interact with DNA and that the homodimer is the relevant DNA-binding species.

We designed experiments to estimate the stability of the dimers according to the reaction

$$2P \underset{K}{\rightleftarrows} P_2$$

where $P$ represents the concentration of monomers and $P_2$ is the concentration of dimers. At equilibrium, $K = [P_2]/[P]^2$ is the dissociation constant of dimers. For the experiments, increasing concentrations of rIBR were incubated for 30 min prior to addition of a constant excess of the PAL probe, and the amount of protein-DNA complex formed at equilibrium was measured by gel retardation assays. Since the DNA was in excess, the concentration of dimers at each protein input was estimated to be equal to the concentration of the DNA complex [$P_2D$], and the monomer concentration was calculated by subtracting the dimer concentration from the total protein concentration. The apparent dissociation constant, calculated from the slope of the plot of $P_2D$ versus $[P]^2$ (Fig. 11A), varied between $4.3 \times 10^{-8}$ and $7.6 \times 10^{-8}$ M in different experiments. Since our approach underestimates the dimer concentration, the actual dissociation constant should be even lower than that calculated. In any case, the result indicates that the dimer is very stable and suggests that, unless properly destabilized, the IBR/F dimer may not easily exchange subunits with other as yet unknown factors (see Discussion).

**Kinetics of DNA binding by IBR.** The equilibrium dissociation constant for the optimal palindrome TGCGCATGCGCA has recently been reported for α-Pal as $6.5 \times 10^{-11}$ M (18), a value which is of the same order of magnitude as the one that we determined for IBR (not shown). Competition experiments indicated that the affinity of IBR for site C/D of *h5* (Fig. 3) and the half-palindrome TGCGCA was 10-fold lower than for the 12-bp palindrome (not shown; see Fig. 10B). Thus, although the contacts determining the stability of the IBR-DNA complex probably occur between each monomer and the CGC/GCG sequences surrounding the central RY dyad, the results indicate that insofar as one of the subunits establishes specific contacts with DNA, the other subunit can accommodate a variety of other sequences at a relatively low thermodynamic cost for the complex.

To characterize the kinetics of IBR interaction with those sequences, the apparent association and dissociation rates of the DNA complexes were determined. Surprisingly, the apparent association rate to the palindrome was between 1.6 and 1.8 times slower than that to the *h5* sequence (Fig. 11C). Since the effect was reproducible, the result may indicate that stable binding of IBR to the palindrome requires a structural transition to occur in the complex, a transition which may not occur in the imperfect *h5* sequence. On the other hand, the half-life of the *h5* complex was 15 times shorter than that of the palindrome complex, the $t_{1/2}$ of the palindrome and *h5* complex being 38 and 2.5 min, respectively (Fig. 11B). The high off-rate of the *h5* complex suggests that the transcriptional effect of IBR on the *h5* promoter should be highly sensitive to the intracellular concentration of the factor.

**DNA-binding and dimerization domains of IBR.** To dissect the functional domains of IBR, a series of N- and C-terminal deletion mutants (summarized in Fig. 12A) were expressed in *E. coli*. The recombinant proteins were efficiently synthesized in bacteria (Fig. 12B) and soluble under nondenaturing conditions. The DNA-binding activity of the purified proteins was analyzed by gel retardation assays with the PAL probe, whereas their ability to form dimers was assessed in parallel experiments by glutaraldehyde cross-linking. Mutant ΔN110 was not included in this study because the majority of molecules were cleaved at an internal site in *E. coli* (Fig. 12B). The results of the gel retardation assays (Fig. 12C) indicated that all mutants except ΔN172 and ΔC247 were able to form complexes ΔN79, which is not shown in the figure, was also able to form a complex). Therefore, the outer limits of the DNA-binding/dimerization domain, which comprises most of the evolutionarily conserved region, is defined by deletions ΔN127 and ΔC283 (Fig. 12A and C). Glutaraldehyde cross-linking indicated that all the mutants except ΔN172 efficiently formed dimers (not shown). The ΔN172 monomer was cross-linked into higher-order oligomers with no pause at the dimeric form, indicating the lack of a definite complex. These results, summarized in Fig. 12A, locate the dimerization domain towards

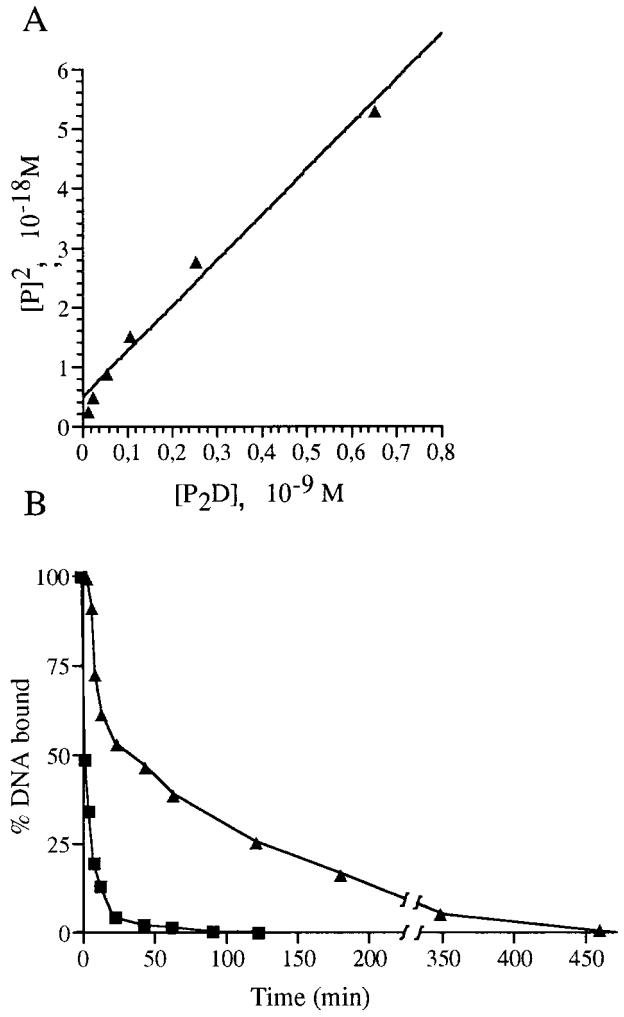


FIG. 11. Kinetic measurements of IBR binding to DNA. (A) Determination of the dissociation constant of rIBR dimers into monomers. (B) Dissociation rates of the IBR-PAL (▲) and IBR-*h5* (■) complexes. (C) Association rates of IBR to PAL (▲) and *h5* probes (■).

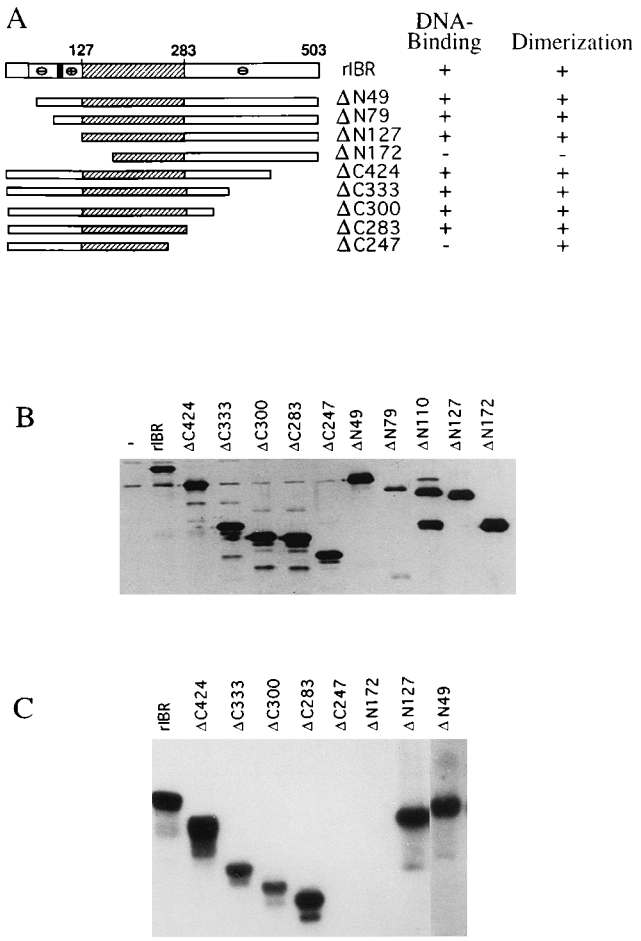


FIG. 12. Deletion mapping of IBR. (A) Diagram of the deletion mutants of IBR tested for dimerization and DNA binding. The 127 to 283 box indicates the outer limits of the DNA-binding/dimerization domain. (B) Western blot of whole *E. coli* BL21(DE3) expressing the indicated IBR mutants reacted with anti-rIBR antibodies. Lane —, nontransformed BL21(DE3). (C) DNA-binding activity of IBR deletion mutants. The $^{32}$P-labeled PAL probe was used for the gel retardation assays. Only the region containing the complexes is shown.

the N-terminal region of the composite DNA-binding/dimerization domain.

The DNA-binding domain of IBR, which is relatively proline-rich and neutral in charge, shows none of the typical motifs found in other transcription factors, including zinc fingers, b-ZIP, basic helix-loop-helix, and helix-turn-helix. The region encompassing residues 232 to 255 has the loose consensus of a homeobox domain signature. However, it is unlikely that a typical helix-turn-helix can be formed because the region that should correspond to helix II (24) is punctuated with proline residues and therefore cannot adopt an α-helix conformation.

**Nuclear targeting of IBR.** We examined whether the evolutionarily conserved bipartite NLS which lies at the N-terminal side of the dimerization/DNA-binding domain (Fig. 2 and 4) was functional. Transformed H32 quail fibroblasts were transfected with RSV vectors expressing the collection of IBR deletion mutants described above, and the cellular compartmentalization of the proteins was determined by indirect immunofluorescence and confocal microscopy. The primary antibody used for detection of the N-terminal deletion mutants was directed against an SV40 T antigen epitope tag (49) introduced at the C terminus of IBR. To detect the C-terminal deletion mutants,

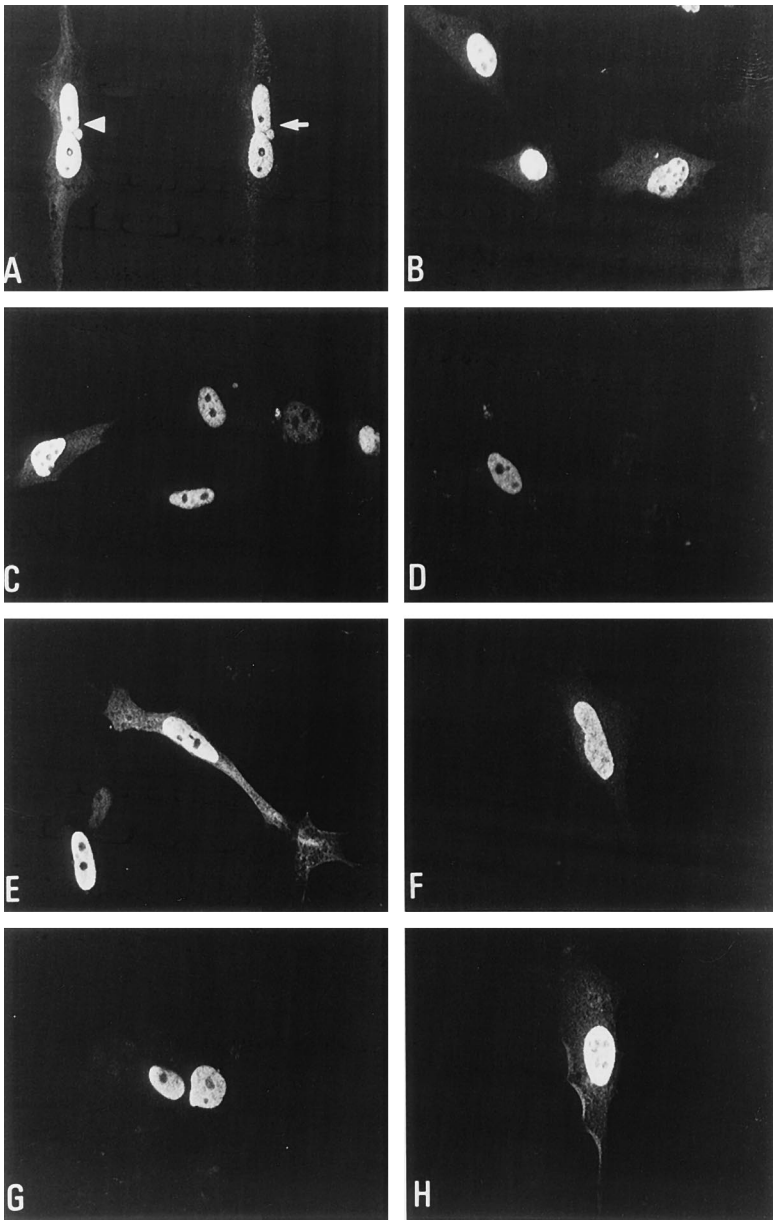


FIG. 13. Cellular localization of IBR and IBR deletion mutants by indirect immunofluorescence. H32 cells transfected with the indicated IBR expression vectors were reacted with mouse monoclonal antibody kt3 (A to C) or affinity-purified rabbit anti-rIBR antibodies (A and D to H) and postreacted with fluorescein isothiocyanate-conjugated anti-mouse IgG or Texas red-conjugated anti-rabbit IgG antibodies, respectively. (A) RSV-IBR; the field shows the same cell reacted with kt3 (arrowhead) and anti-rIBR (arrow) antibodies. (B) RSV-ΔN49; (C) RSV-ΔN79; (D) RSV-ΔC434; (E) RSV-ΔC333; (F) RSV-ΔC300; (G) RSV-ΔC283; (H) RSV-ΔC247. See Fig. 12A for maps of the deletion mutants.

diluted anti-rIBR was used as the primary antibody because a short FLAG epitope tag (6), introduced at the N terminus of IBR, was not recognized by the commercial antibodies. The results indicated that the antibodies specifically recognized the presence of the transgenic IBR and that, in the case of anti-rIBR, the endogenous factor did not interfere with the analysis because of its lower relative concentration with respect to that of the transgenic proteins (however, when the concentration of anti-rIBR antibodies was increased 20-fold, the nontransfected cells showed the same type of nuclear fluorescence as the transfected cells, and no fluorescence was detected if the antibodies were preincubated with rIBR). Figure 13A shows a transfected cell expressing transgenic IBR reacted either with the monoclonal antibody against the T antigen epitope (arrowhead, green fluorescence in the original) or with diluted affinity-purified anti-rIBR (arrow, red fluorescence in the original). The two antibodies gave intense granular nuclear fluorescence and the nucleoli were negative, whereas the nontransfected cells present in the preparation showed no nuclear fluorescence (see, for example, Fig. 13B). Deletion of residues 1 to 49 (Fig. 13B) and 1 to 79 (Fig. 13C) at the N terminus did not affect the nuclear localization of the proteins, whereas mutations removing sequences 1 to 127 and 1 to 172 resulted in lack of nuclear fluorescence (not shown), even though control experiments indicated that the cells had been transfected. Since the ΔN127 and ΔN172 mutants also failed to accumulate in the

cytoplasm, the results indicate that deletion of residues 79 to 127 removed the nuclear targeting sequence and/or destabilized the proteins. On the other hand, removal of C-terminal sequences from 503 to 424, 333, 300, 283, and 247 produced proteins that localized in the nucleus (Fig. 13D to H). These results argue that the bipartite NLS, encompassing residues 89 to 106, is necessary for nuclear targeting of IBR.

## DISCUSSION

**Cloning of IBR cDNA.** To characterize IBR, we have isolated its cDNA from a chicken erythrocyte library. The results indicate that pcIBR encodes IBR. (i) The ORF included the sequences of the four peptides obtained from purified IBR. (ii) The recombinant protein had the expected size, gave identical footprints to IBR on the *h5* promoter, and formed complexes with DNA having the same electrophoretic mobility as IBR. (iii) Anti-IBR IgG recognized the recombinant protein and vice versa. (iv) The peptides produced from IBR and rIBR by cleavage at tryptophan residues had identical electrophoretic mobilities.

The predicted sequence of IBR indicated that the factor is a member of a family of evolutionarily related factors that includes sea urchin P3A2 (11), *Drosophila* EWG (17), and human NRF-1/α-Pal (18, 88). In fact, IBR/F and NRF-1/α-Pal are 99% identical in sequence.

**Relationship of IBR with IBF.** We have shown that IBR from erythrocytes and IBF from HD3 cells are products of the same gene that most likely have the same amino acid sequence. (i) Partial IBF cDNAs had sequences identical to IBR cDNA (unpublished observations). (ii) The IBR gene is single copy. (iii) The IBR cDNA hybridized to a $3.6 \times 10^3$ nucleotide-long RNA from erythrocytes (containing IBR but not IBF) and HD3 cells (containing IBF but not IBR). (iv) IBR and IBF gave identical footprints on the *h5* promoter and formed complexes with DNA having the same electrophoretic mobilities. (v) IBF and NRF-1 had the same electrophoretic mobility and were recognized by anti-IBR and anti-rIBR IgG. (vi) The peptides produced by cleavage of IBR and IBF at tryptophan residues had the same electrophoretic mobilities.

Although we cannot completely rule out that IBR and IBF are the products of alternative splicing differing by the presence or absence of a short peptide sequence, our evidence and the independent cloning of the human cDNAs for NRF-1 (88) and α-Pal (18), which predicts a protein of the same size and essentially the same sequence as IBR, do not support this possibility.

**Posttranslational modifications of IBR and IBF.** We have shown that the difference in apparent molecular mass between IBR and IBF is probably due to the differential glycosylation of these factors. Purified IBR but not IBF was able to bind succinylated WGA, which is specific for *N*-acetylglucosamine (GlcNAc) residues. Although the nature of the glycosidic linkage was not determined, we presume, by analogy to other glycosylated intracellular proteins (30), that several monosaccharide moieties are linked to hydroxyl groups of serine or threonine residues (O-GlcNAc). The IBR glycosylated form appears to specifically occur in maturing and mature adult erythrocytes, whereas the apparently nonglycosylated IBF form was found in earlier erythroid precursors and other types of cells (liver, brain, MSB-1, HeLa, NIH 3T3, and L cells) from several vertebrates (human, mouse, rat, and chicken).

O-GlcNAc glycosylation of transcription factors has been extensively documented in the cases of Sp1 (38) and serum response transcription factor (SRF) (68). In vitro assays indicated that SRF glycosylation plays no major role in DNA binding (50, 53). In the case of Sp1, the nonglycosylated recombinant protein was able to bind to DNA but showed reduced ability to transactivate (38). However, it is not clear whether this was due to the lack of glycosylation, lack of phosphorylation, or to an anomalous structure of the bacterial protein. In the case of IBR/F, glycosylation does not appear to alter its ability to dimerize and bind to DNA (this work) or to detectably influence its transcriptional effect on the *h5* and model promoters in vitro (24a). These results notwithstanding, we cannot exclude that IBR glycosylation affects its transcriptional properties in other promoter contexts. For example, the steric effects of the sugar moieties or inhibition of phosphorylation at the glycosylated sites (41) could modulate its interactions with certain ancillary transcription factors.

We have also shown that IBR/F is phosphorylated in vivo and that CK-II phosphorylates in vitro at least one of four putative sites in the region extending from residues 37 to 67. With the caveat that phosphorylation in vitro and in vivo could be unrelated (37), the fact that the sites occur in an evolutionarily conserved region suggests that this modification may have a functional role. CK-II is an essential Ser/Thr protein kinase, the activity of which is higher in tissues of elevated metabolic activity (37). Because no second messengers for CK-II are known (37), it is difficult to relate its action to a signal transduction pathway. Phosphorylation by CK-II may alter the DNA-binding turnover of IBR/F, as in the case of SRF (53), Max/Myc, and Max/Max (8), or modulate its transcriptional activity, as in the cases of vesicular stomatitis virus phosphoprotein P (4) and the coactivator PC4 (23). CK-II phosphorylation of sites close to the NLS sequence of the SV40 T antigen increase the rate of its nuclear translocation (70), and it is perhaps relevant that the NLS of IBR/F lies close to the CK-II sites.

**Molecular properties of IBR/F.** A comparison of IBR/F with the related factors indicates that the half N-terminal region has been evolutionarily conserved between the vertebrate and invertebrate members of the family. This region harbors a CK-II site(s), the putative NLS, and the DNA-binding/dimerization domain. On the other hand, the C-terminal halves have only conserved short patches of homology.

We have presented direct evidence that IBR/F associates as stable dimers in solution and that the dimer is the active DNA-binding species. Although this result appears to be at variance with the report that NRF-1 binds to DNA as a monomer (88), that conclusion was reached from the inability of DNA-binding NRF-1 deletion mutants to form heterodimers, an observation which is in agreement with our own results from similar experiments with IBR/F (unpublished observations). However, the failure to heterodimerize under the conditions assayed is an expected consequence of the low equilibrium dissociation constant of the homodimers.

We have delimited the outer borders of the DNA-binding/dimerization domain to the region extending from residues 127 to 283 and shown that the dimerization domain is located at the N-terminal side of the composite domain. These results are in accordance with the deletion analysis of NRF-1 (88), which delimited the outer borders of the DNA-binding domain to the region extending from 105 to 305, since mutants lacking residues 1 to 144 or 503 to 264 were unable to bind to DNA. Taking together the IBR/F and NRF-1 deletion data, it can be concluded that the dimerization domain of these factors starts somewhere between residues 127 and 144 and that the DNA-binding domain ends somewhere between residues 264 and 283.

The DNA-binding/dimerization domain of IBR/F shows none of the typical motifs found in transcription factors, such

as zinc fingers, b-ZIP, or bHLH, since the atypical b-ZIP region proposed for α-Pal (18) was dispensable for both dimerization and DNA binding of the ΔN127 IBR mutant. An analysis of the domain with algorithms for prediction of secondary structure hints that the regions most likely to adopt an α-helix conformation are confined to residues 160 to 175 and 240 to 283, the latter having some resemblance to the DNA-binding helix III of the homeodomain (24). At this stage, we do not know whether the homology is relevant, and structural work will be needed to clarify this issue.

Transcription factors very often exist as families of related members that recognize identical or similar DNA sequences. The families may originate from the same gene by alternative splicing or alternative polyadenylation, for example, ATF/CREB (28) and E12/E47 (83), and/or from related genes coding for partially homologous proteins, such as NF-1 (76), GATA (93), and Sp1 (27). Family members can usually be distinguished by their different mRNA sizes or by the distinct electrophoretic mobilities of their complexes with DNA. Using a variety of nuclear extracts, we have not been able to detect specific DNA complexes other than those made by IBR/F. These results, together with other data presented in this work and the lethal phenotype of the *ewg* null mutants (17), raise the interesting possibility that, in a given species, there might be no other highly related family members acting at the same sequences. Moreover, the high stability of the IBR/F homodimer makes the likelihood of subunit exchange with possible partners somehow remote, thus further restricting, although not eliminating, another potential source of functional diversity.

**Possible roles of IBR/F.** To gain wider insight into the genes that might be regulated by IBR/F, a homology search of the GenBank database was carried out with the alternating purine-pyrimidine IBR/F consensus and the restrictive proviso that the sequence should appear no farther than 300 bp upstream from the transcription initiation site. Although the presence of the IBR/F cognate sequence is not a proof of its activity, we noticed in a significant number of cases that the sequence and its location have been evolutionarily conserved, arguing for its functionality. This analysis revealed a set of 88 genes (the list of which, with the locations of the putative IBR/F sites, is available upon request), some of which are known to be regulated by IBR/NRF-1/α-Pal (9, 13, 19, 22, 35, 39, 75).

Interestingly, the palindrome TGCGCATGCGCA was present in only two of the scored genes (31, 32) whereas it did not occur in the genes known to be regulated by this family of factors (9, 13, 19, 22, 25, 35, 39). This indicates that high-affinity sites do depart from the perfect palindrome, in accordance with our binding-site selection data. With a few exceptions, the overwhelming majority of scored genes were TATA-less genes coding for housekeeping enzymatic activities expressed in most tissues, although at various levels. Examples include genes involved in signal transduction (insulin-like growth factor receptor I [14], c-Ha-*ras* [48], $G\alpha_0$ [47], $Ca^{2+}$-binding proteins [3, 29, 43], the regulatory subunit of phosphatase 2A [55], and cyclic nucleotide phosphodiesterase [46]), mitochondrial energy transduction (cytochrome *c* and several subunits of cytochrome *c* oxidase [13, 19, 88], 5-aminolevulinate synthase [5-ALAS] [9], and subunit γ of ATPase/synthase [13, 54]), protein metabolism (subunits α and β of the translation initiation factor eIF-2 [13, 18, 39], the S16 ribosomal protein [89], disulfide isomerase [86], and proteases specific for short-lived or defective proteins, such as the proteasome HC3 [84] and the calcium-activated neutral protease [31]), lipid metabolism (subunit E1α of the mitochondrial pyruvate dehydrogenase [52], sterol and androgen carrier proteins [65, 80], lipoprotein receptor [22], acetyl coenzyme A binding protein [51], carbonyl reductase [20], and alcohol dehydrogenase [7]), and nucleic acid metabolism (DNA polymerase α [63], the 14.5-kDa subunit of RNA polymerase II [1], topoisomerase I [45], mitochondrial transcription factor A [mTFA] [61], inosine-5′-monophosphate dehydrogenase type II [94], hypoxanthine phosphoribosyltransferase [56], glutamine phosphoribosylpyrophosphate amidotransferase [GPAT] and 5′-phosphoribosylaminoimidazole carboxylase [AIRC] [10], GADD153 [62], ERCC2 [90], RNase MRP [12, 58], U2af-binding protein [32], retinoblastoma [85], prohibitin [60], cyclin B1 [66], and RCC1 [21]). In addition to housekeeping functions, IBR/F may also regulate tissue-specific genes in certain types of cells, including *h5* (25), c-*myb* (26, 40), preproenkephalin A (87), synapsin I (77), acetylcholine receptor (33), and slow sarcoplasmic reticulum Ca-dependent ATPase (71).

Although more functional data are needed, it appears possible that IBR/F and related factors are primarily involved in the coregulation of networks of genes involved in growth-related functions. Therefore, to unify the present nomenclatures, we would like to propose the more general term GRF-1 (growth regulatory factor 1) to describe IBR/F and related factors because it appears to portray their functions more appropriately than the current particular definitions.

## ACKNOWLEDGMENTS

We are grateful to K. Stone and K. Williams for peptide sequence determination, F. Calzone for kindly providing a chicken P3A2 PCR probe, J. Guay for the MAP kinase tests, J. Renaud for supershift analysis, C. Chamberlain for confocal microscopy, and M. Lambert for oligonucleotide synthesis.

A.G.-C. is a graduate student of the C.I.D. (C.S.I.C. of Barcelona) and was supported by a predoctoral studentship from the Generalitat de Catalunya (Formació d'Investigadors). M.M. was supported by a studentship of the Government of Quebec (Programme de Bourses d'Excellence). The research was supported in part by a grant from the Medical Research Council of Canada.

## REFERENCES

1. **Acker, J., M. Wintzerith, M. Vigneron, and C. Kedinger.** 1993. Structure of the gene encoding the 14.5 kDa subunit of human RNA polymerase II. Nucleic Acids Res. **21:**5345–5350.
2. **Affolter, M., J. Côté, J. Renaud, and A. Ruiz-Carrillo.** 1987. Regulation of histone and $\beta^A$-globin gene expression during differentiation of chicken erythroid cells. Mol. Cell. Biol. **7:**3663–3672.
3. **Banville, D., and Y. Boie.** 1989. Retroviral long terminal repeat is the promoter of the gene encoding the tumor-associated calcium-binding protein oncomodulin in the rat. J. Mol. Biol. **207:**481–490.
4. **Barik, S., and A. K. Banerjee.** 1992. Phosphorylation by cellular casein kinase II is essential for transcriptional activity of vesicular stomatitis virus phosphoprotein P. Proc. Natl. Acad. Sci. USA **89:**6570–6574.
5. **Bates, D. L., and J. O. Thomas.** 1981. Histones H1 and H5: one or two molecules per nucleosome? Nucleic Acids Res. **9:**5883–5894.
6. **Blanar, M. A., and W. J. Rutter.** 1992. Interaction cloning: identification of a helix-loop-helix zipper protein that interacts with c-Fos. Science **256:**1014–1018.
7. **Bodmer, M., and M. Ashburner.** 1984. Conservation and change in the DNA sequences coding for alcohol dehydrogenase in sibling species of *Drosophila*. Nature (London) **309:**425–430.
8. **Bousset, K., M. Henriksson, J. M. Luscher-Firzlaff, D. W. Litchfield, and B. Luscher.** 1993. Identification of casein kinase II phosphorylation sites in Max: effects on DNA-binding kinetics of homo- and Myc/Max heterodimers. Oncogene **8:**3211–3220.
9. **Braidotti, G., I. A. Borthwick, and B. K. May.** 1993. Identification of regulatory sequences in the gene for 5-aminolevulinate synthase from rat. J. Biol. Chem. **268:**1109–1117.
10. **Brayton, K. A., Z. Chen, G. Zhou, P. L. Nagy, A. Gavalas, J. M. Trent, L. L. Deaven, J. E. Dixon, and H. Zalkin.** 1994. Two genes for de novo purine nucleotide synthesis on human chromosome 4 are closely linked and divergently transcribed. J. Biol. Chem. **269:**5313–5321.
11. **Calzone, F. J., C. Hoog, D. B. Teplow, A. E. Cutting, R. W. Zeller, R. J. Britten, and E. H. Davidson.** 1991. Gene regulatory factors of the sea urchin embryo. I. Purification by affinity chromatography and cloning of P3A2, a novel DNA-binding protein. Development **112:**335–350.

12. **Chang, D. D., and D. A. Clayton.** 1989. Mouse RNase MRP RNA is encoded by a nuclear gene and contains a decamer sequence complementary to a conserved region of mitochondrial RNA substrate. Cell **56:**131–139.
13. **Chau, C. M. A., M. J. Evans, and R. C. Scarpulla.** 1992. Nuclear respiratory factor 1 activation sites in genes encoding the γ-subunit of ATP synthase, eukaryotic initiation factor 2α, and tyrosine aminotransferase: specific interaction of purified NRF-1 with multiple target genes. J. Biol. Chem. **267:** 6999–7006.
14. **Cooke, D. W., L. A. Bankert, C. T. Roberts, D. Leroith, and S. J. Casella.** 1991. Analysis of the human type-I insulin-like growth factor receptor promoter region. Biochem. Biophys. Res. Commun. **177:**1113–1120.
15. **Côté, J., and A. Ruiz-Carrillo.** 1993. Primers for mitochondrial DNA replication generated by endonuclease G. Science **261:**765–769.
16. **Crimmins, D. L., D. W. McCourt, R. S. Thoma, M. G. Scott, K. Macke, and B. D. Schwartz.** 1990. In situ chemical cleavage of proteins immobilized to glass-fiber and polyvinylidenedifluoride membranes: cleavage at tryptophan residues with 2-(2′-nitrophenylsulfenyl)-3-methyl-3′-bromoindolenine to obtain internal amino acid sequence. Anal. Biochem. **187:**27–38.
17. **DeSimone, S. M., and K. White.** 1993. The *Drosophila* erect wing gene, which is important for both neuronal and muscle development, encodes a protein which is similar to the sea urchin P3A2 DNA binding protein. Mol. Cell. Biol. **13:**3641–3649.
18. **Efiok, B. J. S., J. A. Chiorini, and B. Safer.** 1994. A key transcription factor for eukaryotic initiation factor-2α is strongly homologous to developmental transcription factors and may link metabolic genes to cellular growth and development. J. Biol. Chem. **269:**18921–18939.
19. **Evans, M. J., and R. C. Scarpulla.** 1990. NRF-1: a trans-activator of nuclear-encoded respiratory genes in animal cells. Genes Dev. **4:**1023–1034.
20. **Forrest, G. L., S. Akman, J. Doroshow, H. Rivera, and W. D. Kaplan.** 1991. Genomic sequence and expression of a cloned human carbonyl reductase gene with daunorubicin reductase activity. Mol. Pharmacol. **40:**502–507.
21. **Furuno, N., K. Nakagawa, U. Eguchi, M. Ohtsubo, T. Nishimoto, E. Soeda, and M. O. Ohtubo.** 1991. Complete nucleotide sequence of the human RCC1 gene involved in coupling between DNA replication and mitosis. Genomics **11:**459–461.
22. **Gaeta, B. A., I. Borthwick, and K. K. Stanley.** 1994. The 5′-flanking region of the α-2MR/LRP gene contains an enhancer-like cluster of SP1 binding-sites. Biochim. Biophys. Acta **1219:**307–313.
23. **Ge, H., Y. Zhao, B. T. Chait, and R. G. Roeder.** 1994. Phosphorylation negatively regulates the function of coactivator PC4. Proc. Natl. Acad. Sci. USA **91:**12691–12695.
24. **Gehring, W. J.** 1992. The homeobox in perspective. Trends Biochem. Sci. **17:** 277–280.

24a. **Gómez-Cuadrado, A., M. Batchvarova, and A. Ruiz-Carrillo.** Unpublished data.

25. **Gómez-Cuadrado, A., S. Rousseau, J. Renaud, and A. Ruiz-Carrillo.** 1992. Repression of the H5 histone gene by a factor from erythrocytes that binds to the region of transcription initiation. EMBO J. **11:**1857–1866.
26. **Graf, T.** 1992. Myb: a transcriptional activator linking proliferation and differentiation in hematopoietic cells. Curr. Opin. Genet. Dev. **2:**249–255.
27. **Hagen, G., S. Muller, M. Beato, and G. Suske.** 1992. Cloning by recognition site screening of two novel GT box binding proteins: a family of SP1 related genes. Nucleic Acids Res. **20:**5519–5525.
28. **Hai, T., F. Liu, W. J. Coukos, and M. R. Green.** 1989. Transcription factor ATF cDNA clones: an extensive family of leucine zipper proteins able to selectively form DNA-binding heterodimers. Genes Dev. **3:**2083–2090.
29. **Hardin, S. H., C. D. Carpenter, P. E. Hardin, A. M. Bruskin, and W. H. Klein.** 1985. Structure of the *Spec1* gene encoding a major calcium-binding protein in the embryonic ectoderm of the sea urchin *Strongylocentrotus purpuratus*. J. Mol. Biol. **186:**243–255.
30. **Hart, G. W., R. S. Haltiwanger, G. D. Holt, and W. G. Kelly.** 1989. Glycosylation in the nucleus and cytoplasm. Annu. Rev. Biochem. **58:**841–874.
31. **Hata, A., S. Ohno, Y. Akita, and K. Suzuki.** 1989. Tandemly reiterated negative enhancer-like elements regulate transcription of a human gene for large subunit of calcium-dependent protease. J. Biol. Chem. **264:**6404–6411.
32. **Hayashizaki, Y., H. Shibata, S. Hirotsune, H. Sugino, Y. Okazaki, N. Sasaki, K. Hirose, H. Imoto, H. Okuizumi, M. Muramatsu, et al.** 1994. Identification of an imprinted U2af binding protein related sequence on mouse chromosome 11 using the RLGS method. Nat. Genet. **6:**33–40.
33. **Hess, N., B. Merz, and E. D. Gundelfinger.** 1994. Acetylcholine receptors of the *Drosophila* brain: a 900 bp promoter fragment contains the essential information for specific expression of the *ard* gene *in vivo*. FEBS Lett. **346:** 135–140.
34. **Howe, L. R., S. J. Leevers, N. Gómez, S. Nakielny, P. Cohen, and C. J. Marshall.** 1992. Activation of the MAP kinase pathway by the protein kinase raf. Cell **71:**335–342.
35. **Humbelin, M., B. Safer, J. A. Chiorini, J. W. B. Hershey, and R. B. Cohen.** 1989. Isolation and characterization of the promoter and flanking regions of the gene encoding the human protein-synthesis-initiation factor 2α. Gene **81:**315–324.
36. **Hunter, T., and M. Karin.** 1992. The regulation of transcription by phosphorylation. Cell **70:**375–387.
37. **Issinger, O.-G.** 1993. Casein kinases: pleiotropic mediators of cellular regulation. Pharmacol. Ther. **59:**1–30.
38. **Jackson, S. P., and R. Tjian.** 1988. O-glycosylation of eukaryotic transcription factors: implication for mechanisms of transcriptional regulation. Cell **55:**125–133.
39. **Jacob, W. F., T. A. Silverman, R. B. Cohen, and B. Safer.** 1989. Identification and characterization of a novel-transcription factor participating in the expression of eukaryotic initiation factor 2α. J. Biol. Chem. **264:**20372–20384.
40. **Jacobs, S. M., K. M. Gorse, and E. H. Westin.** 1994. Identification of a second promoter in the human c-myb proto-oncogene. Oncogene **9:**227–235.
41. **Kearse, K. P., and G. W. Hart.** 1991. Lymphocyte activation induces rapid changes in nuclear and cytoplasmic glycoproteins. Proc. Natl. Acad. Sci. USA **88:**1701–1705.
42. **Kho, C. J., and H. Zarbl.** 1992. A rapid and efficient protocol for sequencing plasmid DNA. Biotechniques **12:**228–230.
43. **Koller, M., B. Schnyder, and E. E. Strehler.** 1990. Structural organization of the human *CaMIII* calmodulin gene. Biochim. Biophys. Acta **1087:**180–189.
44. **Kozak, M.** 1980. Evaluation of the scanning model for initiation of protein synthesis in eukaryotes. Cell **22:**7–8.
45. **Kunze, N., G. C. Yang, M. Dolberg, R. Sundarp, R. Knippers, and A. Richter.** 1991. Structure of the human type I DNA topoisomerase gene. J. Biol. Chem. **266:**9610–9616.
46. **Kurihara, T., K. Monoh, K. Sakimura, and Y. Takahashi.** 1990. Alternative splicing of mouse brain 2′,3′-cyclic-nucleotide 3′-phosphodiesterase mRNA. Biochem. Biophys. Res. Commun. **170:**1074–1081.
47. **Li, Y., R. Mortensen, and E. J. Neer.** 1994. Regulation of $\alpha_0$ expression by the 5′-flanking region of the $\alpha_0$ gene. J. Biol. Chem. **269:**27589–27594.
48. **Lowndes, N. F., J. Paul, J. Wu, and M. Allan.** 1989. c-Ha-*ras* gene bidirectional promoter expressed in vitro: location and regulation. Mol. Cell. Biol. **9:**3758–3770.
49. **Macarthur, H., and G. Walter.** 1984. Monoclonal antibodies specific for the carboxyl terminus of simian virus 40 large T antigen. J. Virol. **52:**483–491.
50. **Manak, J. R., N. de Bisschop, R. M. Kris, and R. Prywes.** 1990. Casein kinase II enhances the DNA binding activity of serum response factor. Genes Dev. **4:**955–967.
51. **Mandrup, S., R. Hummel, S. Ravn, G. Jensen, P. H. Andreasen, N. Gregersen, J. Knudsen, and K. Kristiansen.** 1992. Acyl-CoA-binding protein/diazepam-binding inhibitor gene and pseudogenes: a typical housekeeping gene family. J. Mol. Biol. **228:**1011–1022.
52. **Maragos, C., W. M. Hutchison, K. Hayasaka, G. K. Brown, and H.-H. Dahl.** 1989. Structural organization of the gene for the E1α subunit of the human pyruvate dehydrogenase complex. J. Biol. Chem. **264:**12294–12298.
53. **Marais, R. M., J. J. Hsuan, C. McGuigan, J. Wynne, and R. Treisman.** 1992. Casein kinase II phosphorylation increases the rate of serum response factor-binding site exchange. EMBO J. **11:**97–105.
54. **Matsuda, C., H. Endo, S. Ohta, and Y. Kagawa.** 1993. Gene structure of human mitochondrial ATP synthase γ-subunit: tissue specificity produced by alternative RNA splicing. J. Biol. Chem. **268:**24950–24958.
55. **Mayer Jaekel, R. E., H. Ohkura, R. Gomes, C. E. Sunkel, S. Baumgartner, B. A. Hemmings, and D. M. Glover.** 1993. The 55 kd regulatory subunit of *Drosophila* protein phosphatase 2A is required for anaphase. Cell **72:**621–633.
56. **Melton, D. W., C. McEwan, A. B. McKie, and A. M. Reid.** 1986. Expression of the mouse HPRT gene: deletional analysis of the promoter region of an X-chromosome linked housekeeping gene. Cell **44:**319–328.
57. **Morrissey, J. H.** 1981. Silver stain for proteins in polyacrylamide gels: a modified procedure with enhanced uniform sensitivity. Anal. Biochem. **117:** 307–310.
58. **Morrissey, J. P., and D. Tollervey.** 1995. Birth of the snoRNPs: the evolution of RNase MRP and the eukaryotic pre-rRNA-processing. Trends Biochem. Sci. **20:**78–82.
59. **Mueller, P. R., and B. Wold.** 1989. In vivo footprinting of a muscle specific enhancer by ligation mediated PCR. Science **246:**780–786.
60. **Nuell, M. J., D. A. Stewart, L. Walker, V. Friedman, C. M. Wood, G. A. Owens, J. R. Smith, E. D. Schneider, R. Dell'Orco, C. K. Lumpkin, D. B. Danner, and J. K. McClung.** 1991. Prohibitin, an evolutionarily conserved intracellular protein that blocks DNA synthesis in normal fibroblasts and HeLa cells. Mol. Cell. Biol. **11:**1372–1381.
61. **Parisi, M. A., and D. A. Clayton.** 1991. Similarity of human mitochondrial transcription factor-1 to high mobility group proteins. Science **252:**965–969.
62. **Park, J. S., J. D. Luethy, M. G. Wang, J. Fargnoli, A. J. J. Fornace, O. W. McBride, and N. J. Holbrook.** 1992. Isolation, characterization and chromosomal localization of the human *GADD153* gene. Gene **116:**259–267.
63. **Pearson, B. E., H. P. Nasheuer, and T. S. Wang.** 1991. Human DNA polymerase α gene: sequences controlling expression in cycling and serum-stimulated cells. Mol. Cell. Biol. **11:**2081–2095.
64. **Perucho, M., H. V. Molgaard, A. Shevack, T. Pataryas, and A. Ruiz-Carrillo.** 1979. An improved method for preparation of undegraded polysomes and active mRNA from immature chicken erythrocytes. Anal. Biochem. **98:**464–471.
65. **Pfeifer, S. M., E. E. Furth, T. Ohba, Y. J. Chang, H. Rennert, N. Sakuragi, J. T. Billheimer, and J. F. Strauss.** 1993. Sterol carrier protein 2: a role in

steroid hormone synthesis? J. Steroid Biochem. Mol. Biol. **47:**167–172.
66. **Piaggio, G., A. Farina, D. Perrotti, I. Manni, P. Fuschi, A. Sacchi, and C. Gaetano.** 1995. Structure and growth-dependent regulation of the human cyclin B1 promoter. Exp. Cell Res. **216:**396–402.
67. **Prats, E., L. Cornudella, and A. Ruiz-Carrillo.** 1989. Nucleotide sequence of a cDNA for $\phi_0$, a histone to protamine transition protein from sea cucumber spermatozoa. Nucleic Acids Res. **17:**10097.
68. **Reason, A. J., H. R. Morris, M. Panico, R. Marais, R. H. Treisman, R. S. Haltiwanger, G. W. Hart, W. G. Kelly, and A. Dell.** 1992. Localization of O-GlcNAc modification on the serum response transcription factor. J. Biol. Chem. **267:**16911–16921.
69. **Renaud, J., and A. Ruiz-Carrillo.** 1986. Fine analysis of the active *h5* gene chromatin of chicken erythroid cells at different stages of differentiation. J. Mol. Biol. **189:**217–226.
70. **Rihs, H. P., D. A. Jans, H. Fan, and R. Peters.** 1991. The rate of nuclear cytoplasmic protein transport is determined by the casein kinase-II site flanking the nuclear localization sequence of the SV40 T-antigen. EMBO J. **10:**633–639.
71. **Rohrer, D. K., R. Hartong, and W. H. Dillmann.** 1991. Influence of thyroid hormone and retinoic acid on slow sarcoplasmic reticulum $Ca^{2+}$ ATPase and myosin heavy chain alpha gene expression in cardiac myocytes: delineation of *cis*-active DNA elements that confer responsiveness to thyroid hormone but not to retinoic acid. J. Biol. Chem. **266:**8638–8646.
72. **Rousseau, S., M. Asselin, J. Renaud, and A. Ruiz-Carrillo.** 1993. Transcription of the histone *h5* gene is regulated by three differentiation-specific enhancers. Mol. Cell. Biol. **13:**4904–4917.
73. **Rousseau, S., J. Renaud, and A. Ruiz-Carrillo.** 1989. Basal expression of the histone *h5* gene is controlled by positive and negative cis-acting sequence. Nucleic Acids Res. **17:**7495–7511.
74. **Rozalski, M., L. Lafleur, and A. Ruiz-Carrillo.** 1985. Monoclonal antibodies against histone H5: epitope mapping and binding to chromatin. J. Biol. Chem. **260:**14379–14385.
75. **Ruiz-Carrillo, A., M. Affolter, and J. Renaud.** 1983. Genomic organization of the genes coding for the six main histones of the chicken: complete sequence of the *h5* gene. J. Mol. Biol. **170:**843–859.
76. **Rupp, R. A. W., U. Kruse, G. Multhaup, U. Gobel, K. Beyreuther, and A. E. Sippel.** 1990. Chicken NFI/GGCA proteins are encoded by at least three independent genes: NFI-A, NFI-B and NFI-C with homologues in mammalian genomes. Nucleic Acids Res. **18:**2607–2616.
77. **Sauerwald, A., C. Hoesche, R. Oschwald, and M. W. Kilimann.** 1990. The 5′-flanking region of the synapsin I gene: a G+C-rich, TATA- and CAAT-less, phylogenetically conserved sequence with cell type-specific promoter function. J. Biol. Chem. **265:**14932–14937.
78. **Schneider, C., R. A. Newman, D. R. Sutherland, U. Asser, and M. F. Greaves.** 1982. A one-step purification of membrane proteins using a high efficiency immunomatrix. J. Biol. Chem. **257:**10766–10769.
79. **Studier, F. W., and B. A. Moffatt.** 1986. Use of bacteriophage T7 RNA polymerase to direct selective high-level expression of cloned genes. J. Mol. Biol. **189:**113–130.
80. **Sullivan, P. M., Y. M. Wang, and D. R. Joseph.** 1993. Identification of an alternate promoter in the rat androgen-binding protein/sex hormone-binding globulin gene that regulates synthesis of a messenger RNA encoding a protein with altered function. Mol. Endocrinol. **7:**702–715.
81. **Sun, J. M., Z. Ali, R. Lurz, and A. Ruiz-Carrillo.** 1990. Replacement of histone H1 by H5 *in vivo* does not change the nucleosome repeat length of chromatin but increases its stability. EMBO J. **9:**1651–1658.
82. **Sun, J. M., R. Wiaderkiewicz, and A. Ruiz-Carrillo.** 1989. Histone H5 in the control of DNA synthesis and cell proliferation. Science **245:**68–71.
83. **Sun, X. H., and D. Baltimore.** 1991. An inhibitory domain of E12 transcription factor prevents DNA binding in E12 homodimers but not in E12 heterodimers. Cell **64:**459–470.
84. **Tamura, T., F. Osaka, Y. Kawamura, T. Higuti, N. Ishida, H. G. Nothwang, C. Tsurumi, K. Tanaka, and A. Ichihara.** 1994. Isolation and characterization of $\alpha$-type HC5 subunit genes of human proteasomes. J. Mol. Biol. **244:**117–124.
85. **T'Ang, A., K.-J. Wu, T. Hashimoto, W.-Y. Liu, R. Takahashi, X.-H. Shi, K. Mihara, F.-H. Zhang, Y. Y. Chen, C. Du, J. Qian, Y.-G. Lin, A. L. Murphree, W.-R. Qiu, T. Thompson, W. F. Benedict, and Y.-K. Fung.** 1989. Genomic organization of the human retinoblastoma gene. Oncogene **4:**401–407.
86. **Tasanen, K., J. Oikarinen, K. I. Kivirikko, and T. Pihlajaniemi.** 1992. Promoter of the gene for the multifunctional protein disulphide isomerase polypeptide: functional significance of the six CCAAT boxes and other promoter elements. J. Biol. Chem. **267:**11513–11519.
87. **Terao, M., Y. Watanabe, M. Mishina, and S. Numa.** 1983. Sequence requirement for transcription in vivo of the human preproenkefalin A gene. EMBO J. **2:**2223–2228.
88. **Virbasius, C. M. A., J. V. Virbasius, and R. C. Scarpulla.** 1993. NRF-1, an activator involved in nuclear-mitochondrial interactions, utilizes a new DNA-binding domain conserved in a family of developmental regulators. Genes Dev. **7:**2431–2445.
89. **Wagner, M., and R. P. Perry.** 1985. Characterization of the multigene family encoding the mouse S16 ribosomal protein: strategy for distinguishing an expressed gene from its processed pseudogene counterparts by an analysis of total genomic DNA. Mol. Cell. Biol. **5:**3560–3576.
90. **Weber, C. A., E. P. Salazar, S. A. Stewart, and L. H. Thompson.** 1990. ERCC2: cDNA cloning and molecular characterization of a human nucleotide excision repair gene with high homology to yeast *RAD3*. EMBO J. **9:** 1437–1447.
91. **Wells, R. D., S. Amirhaeri, J. A. Blaho, D. A. Collier, A. Dohrman, J. A. Griffin, J. C. Hanvey, A. Jaworski, J. E. Larson, A. Rahmouni, M. Rajagopalan, and W. Shimizu.** 1990. Z DNA and triplexes, p. 79–91. *In* F. Richardson and R. Lehman (ed.), Molecular mechanisms in DNA replication and recombination. Wiley-Liss, New York.
92. **Woodward, M. P., W. W. Young, and R. A. Bloodgood.** 1985. Detection of monoclonal antibodies specific for carbohydrate epitopes using periodate oxidation. J. Immunol. Methods **78:**143–153.
93. **Yamamoto, M., L. J. Ko, M. W. Leonard, H. Beug, S. H. Orkin, and J. D. Engel.** 1990. Activity and tissue-specific expression of the transcription factor NF-E1 multigene family. Genes Dev. **4:**1650–1662.
94. **Zimmermann, A. G., J. Spychala, and B. S. Mitchell.** 1995. Characterization of the human inosine-5′-monophosphate dehydrogenase type II gene. J. Biol. Chem. **270:**6808–6814.